American Diabetes Association. diabetes

SUBCUTANEOUS FAT TRANSPLANTATION ALLEVIATES DIET-INDUCED GLUCOSE INTOLERANCE AND INFLAMMATION IN MICE

Journal:	*Diabetes*
Manuscript ID:	Draft
Manuscript Type:	Original Article
Date Submitted by the Author:	n/a
Complete List of Authors:	Hocking, Samantha; Royal North Shore Hospital, Endocrinology; Garvan Institute for Medical Research, Diabetes and Metabolism Division Stewart, Rebecca; Garvan Institute for Medical Research, Diabetes and Metabolism Division Brandon, Amanda; Garvan Institute for Medical Research, Diabetes and Metabolism Division Suryana, Eurwin; Garvan Institute for Medical Research, Diabetes and Metabolism Division Stuart, Ella; Garvan Institute for Medical Research, Diabetes and Metabolism Division Baldwin, Emily; Garvan Institute for Medical Research, Diabetes and Metabolism Division Kolumam, Ganesh; Genentech, Inc, Tumor Biology and Angiogenesis Karsten, Elisabeth; Macquarie University, Department of Chemistry and Biomolecular Science Herbert, Ben; Macquarie University, Department of Chemistry and Biomolecular Science Cooney, Gregory; Garvan Institute for Medical Research, Diabetes and Metabolism Division; University of New South Wales Australia, St. Vincent's Clinical School Swarbrick, Michael; Garvan Institute for Medical Research, Diabetes and Metabolism Division; University of New South Wales Australia, School of Medical Sciences

SUBCUTANEOUS FAT TRANSPLANTATION ALLEVIATES DIET-INDUCED GLUCOSE INTOLERANCE AND INFLAMMATION IN MICE

Authors: Samantha L. Hocking[1,2], Rebecca L. Stewart[1], Amanda E. Brandon[1], Eurwin Suryana[1], Ella Stuart[1], Emily M. Baldwin[1], Ganesh A. Kolumam[3], Elisabeth Karsten[4], Ben J. Herbert[4], Gregory J. Cooney[1,5], and Michael M. Swarbrick[1,6].

Affiliations: [1]Diabetes and Metabolism Division, Garvan Institute of Medical Research, 384 Victoria Street, Darlinghurst 2010, Sydney, NSW, Australia; [2]Department of Endocrinology, Royal North Shore Hospital, St. Leonards 2065, Sydney, NSW, Australia; [3]Tumor Biology and Angiogenesis, Genentech Inc., South San Francisco, California, United States of America; [4]Biomolecular Frontiers Centre, Department of Chemistry and Biomolecular Science, Faculty of Science, Macquarie University 2019, NSW, Australia; [5]St. Vincent's Clinical School, UNSW Medicine, St. Vincent's Hospital, Darlinghurst 2010, Sydney, NSW, Australia; and [6]School of Medical Sciences, Wallace Wurth Building, University of New South Wales Australia, Kensington 2052, NSW, Australia.

Address correspondence to: Michael M. Swarbrick, PhD, Diabetes and Obesity Program, 384 Victoria Street, Darlinghurst 2010 Sydney, Australia.

Tel: +61 2 9295 8310; Fax: +61 2 9295 8201 Email: m.swarbrick@garvan.org.au

Running title: Fat transplantation improves glucose tolerance

Abstract word count: 199 **Text word count:** 4,066

No. of tables: 0 **No. of figures:** 7

No. of supplementary tables: 3 **No. of supplementary figures:** 6

ABSTRACT:

Adipose tissue distribution is a major determinant of human mortality and morbidity. In mice, intra-abdominal transplantation of subcutaneous adipose tissue protects against glucose intolerance and insulin resistance, but the underlying mechanisms are not well understood. Here, we investigate changes in systemic inflammation, adipokines and tissue-specific glucose uptake in male mice implanted intra-abdominally with either inguinal (subcutaneous) or epididymal (visceral) adipose tissue and fed a high-fat diet for up to 17 weeks. Glucose tolerance was improved in mice receiving subcutaneous adipose tissue from 6 weeks after transplantation, and was observed independently of body weight, skeletal muscle glucose uptake, and plasma leptin and adiponectin concentrations. High-fat diet-induced increases in systemic pro-inflammatory cytokines were also markedly suppressed, some from as early as 4 weeks post-transplant. Specifically, early differences in plasma concentrations of tumor necrosis factor-alpha and interleukin-17 concentrations predicted subsequent improvements in glucose tolerance and insulinaemia. Grafted fat displayed a significant increase in glucose uptake and unexpectedly, a marked induction of skeletal muscle gene expression. Consistent with their improved glucose tolerance, mice receiving subcutaneous fat displayed a significant attenuation of high-fat diet-induced hepatic triglyceride accumulation. These findings have implications for our future understanding of the relationship between regional adiposity and metabolic disease.

Abbreviations:

AdipoR2	adiponectin receptor 2
AT	adipose tissue
CCL2/MCP-1	chemokine (C-C motif) ligand 2/monocyte chemotactic protein-1
CCL4/MIP-1β	chemokine (C-C) ligand 2/macrophage inflammatory protein-1 beta
EPI	epididymal
FFA	free fatty acids
Foxa2	forkhead box protein A2
GTT	glucose tolerance test
HFD	high-fat diet
IL	interleukin
ipGTT	intraperitoneal glucose tolerance test
ING	inguinal
IR	insulin resistance
ITT	insulin tolerance test
Lpl	lipoprotein lipase
SAT	subcutaneous adipose tissue
SOCS3	suppressor of cytokine signalling 3
STAT3	signal transducer and activator of transcription 3
SubQ	subcutaneous
T2DM	type 2 diabetes mellitus
TG	triglyceride
TNF-α	tumor necrosis factor-alpha
VAT	visceral adipose tissue
Vis	visceral

Adipose tissue (AT) distribution is a major determinant of mortality and morbidity in humans (1, 2). Specifically, accumulation of intra-abdominal or 'visceral' AT (VAT) is associated with a greater incidence of type 2 diabetes, dyslipidaemia and hypertension (3). This relationship was originally proposed to be due to increased free fatty acid (FFA) flux from enlarged adipocytes VAT to the liver, leading to hepatic triglyceride (TG) accumulation and development of insulin resistance (IR) (4). However, studies in humans have shown that although portal FFA flux from VAT does increase in obesity, it only constitutes ~20% of total portal FFA flux, with the rest derived from the systemic circulation (5).

AT depots are highly heterogeneous (6), differing in their metabolic characteristics, including insulin and catecholamine sensitivity, response to positive energy balance (hypertrophy vs. hyperplasia), innervation, vascularization and production of secreted molecules ('adipokines'). Many of these depot-specific properties are intrinsic, being maintained in adipocytes isolated as precursors and differentiated *in vitro* (7). As these characteristics are often dysregulated in obesity, they may in turn influence the risk of metabolic disease.

In contrast to VAT, greater amounts of subcutaneous adipose tissue (SAT), particularly in the lower body, are associated with a reduced risk of glucose intolerance, IR, dyslipidaemia and atherosclerosis (8). Gluteal-femoral SAT in particular may act as a 'metabolic sink', protecting non-adipose tissues from excessive FFA exposure (9). Once sequestered within this depot, FFAs are relatively resistant to mobilisation (10). Gluteal-femoral SAT also resists deleterious changes in gene expression associated with obesity (11).

Obesity and IR are characterised by chronic inflammation (12), with the involvement of many pro-inflammatory (tumor necrosis alpha (TNF-α), interleukin-6 (IL-6)) and anti-inflammatory (IL-4, IL-13, IL-10) cytokines (13). AT itself is a key site for obesity-induced inflammation: adipocyte hypertrophy is accompanied by macrophage infiltration (14) and

polarisation towards a classically-activated pro-inflammatory (M1) type rather than 'alternatively' activated, anti-inflammatory, (M2) macrophages, which predominate in AT from lean mice (15). M1 macrophages are a major source of pro-inflammatory cytokines in AT, which impair insulin action locally and in other tissues, such as liver (16). AT from obese humans with IR also has a higher pro-inflammatory T-cell content (17). Accordingly, treating inflammation in humans with type 2 diabetes improves glycaemic control (18).

We and others have investigated the relationship between regional adiposity and metabolism by performing syngeneic AT transplantation in mice (19-25). Intra-abdominal transplantation of inguinal SAT (subQ→vis), but not epididymal VAT (vis→vis), improved glucose tolerance and reduced both endogenous and grafted AT mass at 12-13 weeks after surgery, relative to sham-operated controls (19). These findings were confirmed in another study (21), which also reported differences in AT glucose uptake between sham, subQ→vis and vis→vis mice under euglycaemic-hyperinsulinaemic clamp conditions. Vis→vis transplantation produces beneficial effects on glucose tolerance after 4-8 weeks (20, 23); although these were nullified when the grafts were provided with portal drainage (22). Recently, brown AT transplantation has also been reported to improve metabolism (26, 27).

Here we describe the time-course (up to 17 weeks) for the various metabolic effects related to intra-abdominal AT transplantation, and also investigate adipokines, tissue-specific glucose uptake and systemic inflammation. AT transplantation did not significantly affect body weight, skeletal muscle glucose uptake, or plasma leptin and adiponectin. Instead, we provide evidence to show that subQ→vis transplantation causes a broad and sustained suppression of HFD-induced inflammation that precedes and predicts glucose tolerance.

MATERIALS AND METHODS:

***Animals and housing*:** Six week-old male C57BL6/J mice were obtained from Australian BioResources (Moss Vale, NSW, Australia). Mice were group-housed on a 12-hour light/dark cycle at 22°C with free access to water and chow (Gordon's Specialty Stockfeeds, Yanderra, NSW, Australia). Studies were approved by the Garvan Institute/St. Vincent's Hospital Animal Experimentation Ethics Committee, following National Health and Medical Research Council of Australia guidelines.

***Surgical methods*:** Inguinal and epididymal fat pads were dissected from anaesthetized donors and stored in sterile, warmed phosphate-buffered saline until implantation. Recipient littermates were anaesthetized and a midline incision was made in the abdomen. Grafts were sutured onto the peritoneal surface of the anterior abdominal wall using coated Vicryl 4-0 sutures (Ethicon, Somerville, NJ, U.S.A.), and the midline incision closed with wound clips. Sham-operated mice received identical surgical treatment without transplant. After regaining their pre-surgical weight, mice were provided with HFD *ad libitum* (45%, 20%, and 35% of energy from fat, protein and carbohydrates, respectively; 4.7 kcal/g, based on diet #D12451, Research Diets, New Brunswick, NJ, U.S.A). At the time-points stated, mice were sacrificed by cervical dislocation and tissues were dissected, snap-frozen and stored at -80°C.

Intraperitoneal glucose and insulin tolerance tests: Intraperitoneal (*i.p.*) glucose tolerance tests (GTTs) were performed in 6-hour fasted animals using 1.5 or 2 g glucose/kg body weight (depending on experiment) with blood collected from the tail tip. Blood glucose concentrations were measured using an Accu-Chek monitor (Roche Diagnostics, Castle Hill, NSW, Australia). Insulin tolerance tests were performed on fasted mice injected with 0.75 U of insulin/kg body weight *i.p.* (Actrapid, Novo Nordisk, Baulkham Hills, NSW, Australia).

Histological methods and adipocyte size measurements: Tissues were fixed by overnight incubation in 3.7% (v/v) formaldehyde (Fronine Laboratory Supplies, Taren Point, NSW, Australia) at 4°C. Paraffin-embedded tissues were cut into 4 μm sections and stained with hematoxylin and eosin. Three representative non-overlapping images were obtained from each section, and adipocyte size was determined using ImageJ software (National Institutes of Health, U.S.A.) by an investigator blinded to treatment groups.

Biochemical methods: Insulin concentrations were measured using an Ultra Sensitive Mouse Insulin ELISA Kit (Crystal Chem, Downers Grove, IL, USA). Tissue TG and glycogen content were determined as described (28). FFAs were measured in plasma using reagents from Wako Diagnostics (Richmond, VA, U.S.A). Plasma leptin and adiponectin concentrations were measured by ELISA (#90030 Crystal Chem, Downers Grove, IL, U.S.A.; #MRP300, R&D Systems, Minneapolis, MN, U.S.A., respectively). Plasma lactate was measured using a YSI 2300 Analyser (YSI Life Sciences, Yellow Springs, OH, U.S.A.)

Reverse-transcription polymerase chain reaction (RT-PCR): RNA was extracted from liver using TRI reagent (Sigma-Aldrich, St. Louis, MO, U.S.A). Genomic DNA was removed by DNAse I treatment (1 U/5 μg nucleic acid, Promega, Alexandria, NSW, Australia). Reverse transcription was performed using the RT^2 First Strand Kit, and gene expression was measured using Mouse Fatty Liver RT^2 Profiler PCR Arrays (#330231 PAMM-157ZA) and RT^2 Sybr Green qPCR Mastermix (Qiagen, Doncaster, Victoria, Australia). Results were analysed using RT^2 Profiler software, and expression was normalised using both *B2m* (beta-2 microglobulin) and *Gapdh* as housekeeping genes (29).

Immunoblotting: Tissues were homogenized in RIPA buffer (see **Supplementary Methods**). Cleared lysates containing 20 μg protein were electrophoresed in 10% polyacrylamide gels and transferred to PVDF membranes (GE Healthcare, Buckinghamshire, UK). Leptin, AdipoR2 and PPAR-γ antibodies were obtained from Sigma-Aldrich (#L3410,

#SAB1102579) and Biomol (#SA-206, Hamburg, Germany), respectively. SOCS3 (#2923S) and STAT3 (#4904P) antibodies were supplied by Cell Signaling Technology (Danvers, MA, U.S.A.). SREBP-1 and 14-3-3 antibodies (sc-366 and sc-629) were obtained from Santa Cruz Biotechnology (Santa Cruz, CA, U.S.A.). Appropriate HRP-conjugated secondary antibodies were obtained from Jackson ImmunoResearch (West Grove, PA, U.S.A.).

Radiolabelled glucose tolerance tests: Fasted mice were injected with 1.5g/kg glucose *i.p.* containing tracer amounts of U-^{14}C-glucose (10 μCi/mouse) and ^{3}H-2-deoxyglucose (1 μCi/mouse, both from Perkin-Elmer, Glen Waverley, VIC, Australia). Blood was collected from the tail into heparinised tubes (Microvette CB300LH, Sarstedt, Mawson Lakes, SA, Australia) at the timepoints stated. Plasma was separated by centrifuging at 2000x *g* for 5 min at room temperature. Radioactivity of plasma samples was then determined in plasma (10 μL), skeletal muscle (30 mg) and AT (50 mg). Skeletal muscle and AT glucose uptake was determined as described (30).

Tissues for microarray analysis: Tissues for microarray analysis were obtained in our previous study (19), which included mice receiving a subcutaneous inguinal AT graft in the dorsal subcutaneous space (subQ→subQ). RNA was extracted from the following AT depots at 13 weeks after transplantation: subQ→vis and subQ→subQ grafts, endogenous inguinal subcutaneous AT from a subQ→vis recipient (SubQ→vis ING), endogenous epididymal AT from a subQ→vis recipient (SubQ→vis EPI), and inguinal subcutaneous AT from a sham-operated animal (Sham ING). RNA extraction and microarray methods are provided in **Supplementary Methods**.

Measurement of cytokine concentrations: Plasma was collected at 4 and 10 weeks post-transplantation, as above. Freshly-thawed plasma (50 μl) was filtered using sterile Ultrafree-MC GV centrifuge filters (Millipore, Kilsyth, VIC, Australia) and the concentrations of 23 cytokines (see **Supplementary Methods**) were determined using a 96-well Bio-Plex Pro

Mouse Cytokine Assay (#M60-009RDPD) and a Bio-Plex 200 instrument (both from Bio-Rad, Hercules, CA. U.S.A.). The intra-assay %CV for all cytokines was >5%.

Statistical analysis: All data are presented as mean±SEM. Glucose excursions during the GTT (0-120 min) were expressed as incremental area under the curve (iAUC), calculated using Microsoft Excel. Differences between groups were analysed by Student's t-test, 1-way or 2-way ANOVA (or their non-parametric equivalents) using GraphPad Prism 6 Software (GraphPad Software, La Jolla, CA, USA). Multiple comparisons were corrected using the Holm-Sidak (parametric) or Dunn's (non-parametric) tests. Correlations between continuous variables were assessed using Pearson's or Spearman rank, as appropriate. A two-sided $P<0.05$ was considered to be significant.

RESULTS:

1) Glucose tolerance in subQ→vis mice is sustainably improved from 6 weeks post-transplantation. We previously reported beneficial effects of subQ→vis transplantation at 13 weeks (19). Next, we determined the time-course of these effects by studying sham, subQ→vis and vis→vis mice for 3, 6 and 17 weeks (**Figure 1A**). Transplantation did not significantly affect body weight (**Figure 1B**). At sacrifice, there were no significant differences between the masses of endogenous fat depots, although vis→vis grafts were significantly larger than subQ→vis grafts (see below) (**Figure 1C**). Body composition analysis between 6 and 13 weeks post-transplant suggested less fat accretion in subQ→vis mice, but the difference between groups was not significant (**Figure 1D**). Regardless, glucose tolerance was sustainably improved in subQ→vis mice from 6 weeks onwards (**Figure 1E** and **Supplementary Figure 1**). At 7 weeks, subQ→vis mice also displayed the lowest basal and 15 minute blood glucose concentrations during an insulin tolerance test (**Supplementary Figure 2**).

Consistent with the lack of difference in body weight, no detectable differences in energy expenditure or food intake were observed between the groups (**Supplementary Figure 3 and Supplementary Table 1**). As reported previously (21), subQ→vis mice displayed a tendency towards a higher respiratory quotient during the dark phase (**Supplementary Figure 4**).

2) Grafted subcutaneous fat regresses, while grafted visceral fat expands intra-abdominally. Although comparable amounts of AT were initially transplanted into subQ→vis and vis→vis mice (231±10 vs 218±9 mg, P=0.35), grafted epididymal VAT expanded in its new anatomical location, while grafted inguinal SAT reduced its mass

(**Figure 2A**). These divergent effects were apparent at 3 weeks and continued up to 17 weeks, whereupon grafted SAT had reduced to 69% of its initial mass (160±27 mg), while grafted VAT had increased in mass by 169% (587±75 mg, $P<0.0001$). In HFD-fed mice, SAT generally expands by hyperplasia, while VAT displays hypertrophy (31). Expansion of grafted VAT was accompanied by an increase in adipocyte size, while mean cell size decreased slightly in grafted inguinal SAT (**Figures 2B and 2C-H**). Consistent with this finding, vis grafts expressed more leptin (**Figure 2I**). Plasma leptin concentrations only tended to be lower in subQ→vis mice at 17 weeks ($P=0.15$, **Figure 2J**); while adiponectin concentrations were not affected by transplantation (**Figure 2K**).

3) AT glucose uptake is increased following transplantation. To investigate previously-reported improvements in AT (endogenous and grafted) glucose uptake in subQ→vis mice (21), and to account for any contribution of skeletal muscle, we performed radiolabelled glucose tolerance tests in HFD-fed sham, subQ→vis and vis→vis mice at 13 weeks after transplantation. A group of chow mice was included to measure the effects of HFD feeding. As expected, HFD feeding increased adiposity (**Figure 3A**) worsened glucose tolerance (**Figures 3B and C**) and increased fasting insulinaemia (**Figure 3D**).

Remarkably, subQ→vis mice were completely protected against HFD-induced glucose intolerance (**Figure 3C**); and both subQ→vis and vis→vis mice had significantly lower fasting plasma insulin concentrations compared to sham mice (**Figure 3D**). Suppression of plasma FFA concentrations was used as a surrogate measure of adipose insulin sensitivity: FFAs concentrations tended to be highest in sham mice compared to the other groups (**Figure 3E**).

Glucose uptake into quadriceps muscle and all AT depots (intrascapular brown, inguinal, epididymal, retroperitoneal) was reduced by HFD feeding but was not significantly

different between sham, subQ→vis and vis→vis mice (**Figure 3F**). Grafted subQ and vis AT did not differ with respect to glucose uptake (P=0.68); however, when compared to their respective endogenous depots, both subQ and vis adipose tissue grafts showed significantly higher glucose uptake (2.8-fold (P<0.001) and 2.0-fold (P<0.01), respectively). Chronically increasing glucose uptake into AT increases lactate release in the fed state and improves insulin sensitivity (32). Accordingly, subQ→vis mice tended to have higher plasma lactate concentrations than sham mice at 17 weeks after transplantation (**Supplementary Figure 5**).

4) Grafted and endogenous subcutaneous depots of subQ→vis mice display an induction of skeletal muscle-specific genes. To understand the metabolic effects of subQ→vis transplantation, we compared gene expression in subQ grafts that had been implanted into either the abdomen or the dorsal subcutaneous space (subQ→subQ) (**Figure 4A**). SubQ→subQ transplantation does not significantly affect glucose tolerance or adiposity (19); and we expected that any differences in gene expression between subQ→vis and subQ→subQ grafts would be solely due to intra-abdominal transplantation. Twenty-eight genes had a >5-fold increase in expression in subQ→vis compared with subQ→subQ grafts (**Figure 4B**). Many of these genes included cytoskeletal components of skeletal muscle. Gene set enrichment analysis (GSEA) identified a common transcription factor regulating 12 of these genes, myocyte enhancer factor 2A (MEF2A), which plays a key role in skeletal muscle differentiation. Remarkably, expression of these same 12 genes was also increased in the endogenous inguinal AT of subQ→vis mice, relative to sham-operated mice. When the expression of MEF2A, 2B, 2C and 2D was examined in these depots, the endogenous inguinal AT of subQ→vis mice displayed a significant induction of MEF2C and 2D expression (**Figure 4C)**. Interestingly, this coincided with a shift towards smaller adipocyte size in the endogenous inguinal depot of subQ→vis mice (**Figure 4D**).

5) SubQ→vis mice are protected against HFD-induced hepatic TG accumulation. The absence of significant differences in skeletal muscle and endogenous AT glucose uptake between HFD-fed chow, subQ→vis and vis→vis mice led us to also investigate hepatic glucose and lipid metabolism. Relative to vis→vis mice, hepatic TG content was reduced in subQ→vis mice at 17 weeks post-transplantation, but no differences were observed at 6 weeks, when glucose tolerance was first improved (**Figure 5A**). At 17 weeks, hepatic SREBP1 expression also tended to be highest in vis→vis mice relative to either sham or subQ→vis mice (increased 2.22±0.55 fold vs. sham, P=0.12, **Figures 5B** and **5C**).

We also examined the expression of 84 key genes involved in the pathogenesis of nonalcoholic fatty liver disease and hepatic IR (see **Supplementary Figure 6 and Supplementary Table 2**). Livers from subQ→vis mice expressed significantly higher amounts of *Stat3* mRNA than those from vis→vis mice (**Figure 5D**), and tended to have higher amounts than sham livers (increased 1.24-fold, P=0.058). Livers from vis→vis mice displayed a significant down-regulation of *Socs3*, *AdipoR2*, *Lpl*, and *Fox2a* mRNA expression. Differences in mRNA expression were confirmed by immunoblotting: hepatic STAT3 protein expression in subQ→vis and vis→vis mice was 30% and 20% higher than in sham mice, respectively (**Figure 5E**). Differences in hepatic SOCS3, LPL, FOXA2 and ADIPOR2 protein levels were <20% between the three groups. Therefore, the increased TG content in vis→vis mice is likely to be a consequence of increased SREBP1 expression, while increased hepatic STAT3 expression in subQ→vis mice, relative to sham-operated mice, co-incided with improved insulin action.

6) SubQ→vis transplantation reduces circulating markers of inflammation, from as early as 4 weeks post-transplant. HFD-induced obesity and IR are accompanied by chronic inflammation (12). Due to the induction of hepatic STAT3 expression in subQ→vis mice, and its role in inflammatory signalling (33), we performed cytokine profiling in plasma collected from HFD-fed sham, subQ→vis and vis→vis mice at 4 and 10 weeks post-transplantation and at an equivalent time-point in chow-fed mice. Cytokines displaying statistically significant differences between sham, subQ→vis and vis→vis mice are shown in **Figure 6**, and the remainder are shown in **Supplementary Table 3**.

As expected (34), plasma concentrations of the pro-inflammatory cytokines TNF-α and IL-6 were both increased by HFD (**Figure 6A** and **6B**). In subQ→vis mice, however, HFD-induced increases in plasma TNF-α were significantly attenuated at 10 weeks post-transplant. Plasma IL-6 concentrations were markedly elevated in vis→vis mice, but not in subQ→vis mice, at 10 weeks after transplantation (**Figure 6B**).

Obesity also promotes an IL-6 dependent expansion of T helper 17 (Th17) cells, which are a major source of pro-inflammatory IL-17 (35). HFD feeding markedly increased plasma IL-17 concentrations, but this increase was significantly attenuated in subQ→vis mice at both 4 and 10 weeks post-transplantation (**Figure 6C**). HFD-induced increases in plasma concentrations of IL-12p70 and the chemokines MCP-1/CCL5 and MIP-1β/CCL4 have been reported previously (36-38), and were all reduced in subQ→vis mice (**Figures 6D-F**). Plasma concentrations of the Th1 chemokine RANTES were significantly lower in both subQ→vis and vis→vis mice compared to sham mice (**Figure 6G**).

Th2 cells promote anti-inflammatory (M2) macrophage polarization via the production of IL-4, IL-10 or IL-13 (39). Relative to sham-operated mice, concentrations of IL-10 were reduced in subQ→vis and vis→vis mice at 4 weeks; but at 10 weeks, IL-10 was

only suppressed in subQ→vis mice (**Figure 6H**). Transplantation of either type of AT significantly attenuated plasma IL-13 concentrations (**Figure 6I**); while the early reduction in IL-4 due to AT transplantation only persisted in subQ→vis mice (**Figure 6J**). IL-5 is another Th2 cytokine: plasma IL-5 concentrations were increased by HFD feeding and were lower in subQ→vis mice relative to sham mice at both 4 and 10 weeks after transplantation (**Figure 6K**). AT transplantation was also associated with reduced plasma concentrations of the Th1 cytokine IL-2 (**Figure 6L**).

Lastly, we investigated whether concentrations of any of the above cytokines at 4 and 10 weeks predicted either the subsequent response to a glucose tolerance test (iAUC GTT) or fasting insulinaemia at 13 weeks in chow or HFD-fed sham, subQ→vis and vis→vis mice. At 10 weeks post-transplantation, only plasma TNF-α and IL-17 concentrations significantly predicted both iAUC GTT and fasting insulinaemia in the entire set of 40 mice (**Figure 7**). With the exception of IL-6, all cytokines shown in Figure 6 significantly predicted fasting insulinaemia (**Figure 7A**). None of the cytokines measured at 4 weeks post-transplantation significantly predicted subsequent changes in glucose tolerance (data not shown).

DISCUSSION:

SubQ→vis, but not vis→vis, AT transplantation uniquely protects mice against HFD-induced glucose intolerance, hyperinsulinaemia and fat accretion (19, 21, 23, 25). We found that subQ→vis mice developed improved glucose tolerance after 6 weeks, independently of changes in adiposity, or plasma leptin or adiponectin concentrations. Improved glucose tolerance in subQ→vis mice was not explained by increased glucose uptake into skeletal muscle or endogenous AT depots. Grafted AT depots, however, displayed higher glucose uptake than their respective endogenous AT depots, suggesting altered glucose metabolism. Analysis of gene expression in grafts revealed that several targets of the transcription factor MEF2A were upregulated in both the grafted AT and in the endogenous inguinal depots of subQ→vis mice. At later time-points, subQ→vis mice displayed a significant reduction in hepatic TG content, relative to vis→vis mice.

Chronic inflammation makes a key aetiological contribution to diet-induced IR (12). AT from obese mice and humans is characterised by an accumulation of macrophages and their polarization towards a pro-inflammatory (M1) type (14, 15). T-cell recruitment is a primary event in this process, as it precedes AT macrophage infiltration and coincides with the development of IR (40, 41). For example, an increase in the number of CD8+ T-effector cells has been observed in AT as early as 2 weeks after starting HFD feeding (40).

Chronic inflammation has not been extensively investigated in studies of AT transplantation, although isolated measurements have indicated that vis→vis transplantation may exert pro-inflammatory effects. Tran *et al*. (21) reported that vis→vis grafts, but not subQ→vis grafts, displayed an increase in the mRNA expression of *Tnfa* and the macrophage marker *F4/80* relative to endogenous VAT of sham-operated mice, but no plasma cytokine measurements were reported. Elsewhere, in *ApoE*$^{-/-}$ mice, opposing effects of vis→vis and

subQ→vis transplantation on plasma MCP-1 concentrations mice have been reported (24), which are consistent with the present study. One further study has observed a dampening of hepatic gluconeogenic responses when mesenteric fat from IL-1β-deficient mice was transplanted into the abdomen instead of AT from wild-type mice (42). IL-6 has been previously implicated in the deleterious effects of vis→vis transplantation, particularly when epididymal fat was transplanted to the mesenterium instead of the abdominal cavity (22). Our data supports the conclusion that vis→vis transplantation uniquely elevates plasma IL-6 concentrations (**Figure 6B**), but this appears to coincide with glucose intolerance rather than IR *per se*.

Beneficial effects of vis→vis transplantation (with caval drainage not portal) on glucose tolerance have been reported at 4-8 weeks post-transplantation (20, 22, 23). Our time-course studies suggest that in the short term (up to 6 weeks), having an additional AT depot may spare the liver from excessive TG accumulation (**Figure 3A**). In the long term, however, as the grafted VAT hypertrophies, vis→vis transplantation reduces insulinaemia but does not protect against HFD-induced glucose intolerance or fatty liver.

In the present study, we used an unbiased cytokine profiling approach at 2 timepoints to show that subQ→vis transplantation suppressed HFD-induced systemic inflammation. Relative to sham-operated and vis→vis mice, plasma concentrations of TNF-α, IL-17, IL-12p70, MCP-1/CCL2 and MIP-1β/CCL4 were all significantly reduced in subQ→vis mice. Morever, plasma IL-17 and MIP-1β concentrations were suppressed in subQ→vis mice as early as 4 weeks post-transplantation, preceding improvements in glucose tolerance. At 10 weeks post-transplantation, plasma TNF-α and IL-17 concentrations were significantly lower in subQ→vis mice, and predicted both insulinaemia and individual responses to a glucose tolerance test in all mice, irrespective of diet or transplant group (n=40).

The early differences in IL-17 concentrations, and their relationship with subsequent glucose intolerance and insulinaemia, strongly support a role for Th17 cells in the pathogenesis of HFD-induced IR. Diet-induced obesity in C57BL6/J mice is accompanied by a selective expansion of Th17 cells (35). Genetic deletion of IL-17 protects mice against HFD-induced IR and glucose intolerance (43); similarly, neutralization of IL-17 in HFD-fed mice prevents liver injury (44). These findings are relevant for human disease, as IL-17 production from isolated T-cells predicts glycaemic control in humans with diabetes (45).

Elevated IL-17 concentrations are thought to link AT inflammation with hepatic IR. In human SAT, expression of the Th17 master regulator, *RORC*, was positively correlated with that of TNFA and other inflammatory mediators and chemoattractants (46). Pre-treating human hepatocytes with IL-17 inhibits insulin-stimulated Akt phosphorylation and suppression of glucose production (17). Our results strongly suggest that subQ→vis transplantation uniquely suppresses Th17 cell recruitment during diet-induced obesity.

Plasma concentrations of the chemokine MIP-1β were also significantly reduced in subQ→vis mice as early as 4 weeks post-transplantation. MIP-1β has not been well studied in this context, but in young adult humans, plasma MIP-1β concentrations predict waist circumference, independently of age, race, sex and BMI (47).

Differences in immune cell content between epididymal and inguinal AT have been described previously (48). In C57BL6/J mice, epididymal fat is skewed towards innate immunity, while the inguinal depot contains higher proportions of adaptive immune cells (CD4+ and CD8+ T cells and B cells); and the relative proportions of these cells are further altered by HFD feeding (48). Therefore, we hypothesize that subQ→vis transplantation likely prevents HFD-induced glucose intolerance and IR by altering the balance of these cell types *specifically in the intra-abdominal compartment*, as transplantation of an equivalent depot into the subcutaneous space glucose intolerance does not affect glucose tolerance (19, 21).

Characterization of these cell types in grafted fat remains to be investigated in future studies. One important consideration, however, is that cells from donor AT can migrate to other tissues, including lung, liver and spleen, following AT transplantation (49).

Intra-abdominal transplantation of subcutaneous AT produces reproducible beneficial effects on glucose tolerance. Through a combination of time-course studies and unbiased profiling of gene expression and circulating/systemic cytokines, we have identified sustained anti-inflammatory effects that predicted subsequent improvements in glucose tolerance. Future studies will be required to identify the cell type(s) responsible for these effects, and potential sites of intervention for the treatment and prevention of HFD-induced glucose intolerance and IR. Our results significantly enhance our understanding of the relationship between regional adiposity and its deleterious metabolic consequences.

AUTHOR CONTRIBUTIONS:

M.M.S. and S.L.H. designed the experiments. Experiments were performed by M.M.S., R.L.S., S.L.H., A.E.B., E. Suryana and E. Stuart. G.A.K., E.M.B., E.K. and B.J.H. performed tissue analyses. M.M.S compiled data and performed statistical analyses. M.M.S. and S.L.H. wrote the manuscript with input from R.L.S., A.E.B., and G.J.C.

ACKNOWLEDGEMENTS:

This work was supported by Program (to G.J.C.) and Project Grants (to M.M.S., S.L.H. and A.E.B) from the National Health and Medical Research Council (NHMRC) of Australia. The authors would like to thank Paul Lee, Jenny Gunton and Warran Kaplan (Garvan Institute) for their constructive comments on the manuscript, as well as the staff of the Garvan Institute Histopathology (Alice Boulghourjian, Anaiis Zaratzian) and Biological Testing Facilities. M.M.S. takes full responsibility for the work as a whole, including the study design, access to data, and the decision to submit and publish the manuscript.

LEGENDS FOR FIGURES:

Figure 1. Whole-body effects of intra-abdominal adipose tissue transplantation. A. Time-course studies. Male C57BL6/J mice were allocated to weight-matched groups and allowed to acclimatise for one week prior to adipose tissue transplantation (T). Mice regained their pre-surgical weight within 7-10 days and were then provided *ad libitum* with a HFD (45% of calories as fat). Twenty-two mice (8 sham, 6 subQ→vis, 8 vis→vis) were sacrificed after 3 weeks, and twenty-seven mice (10 sham, 7 subQ→vis, 10 vis→vis) were sacrificed at 6 weeks. The remainder (8 sham, 7 subQ→vis, 9 vis→vis) were studied for 17 weeks post-transplantation. Abbreviations for procedures are shown as: GTT, glucose tolerance test; DXA, dual-energy x-ray absorptiometry; ITT, insulin tolerance test; EE, energy expenditure; RQ, respiratory quotient. **B. Effects on body weight.** Results are shown as mean±SEM. There was no significant effect of adipose tissue transplantation on body weight at any of the time-points studied. **C. Individual fat pad weights at 17 weeks post-transplantation.** Results are shown as mean±SEM. Differences between groups were assessed by one-way ANOVA, or t-test for grafts. *** $P<0.001$ vs. subQ→vis mice. **D. Fat mass at 6 and 13 weeks post-transplantation.** DEXA scans (GE Lunar PIXImus) were performed at 6 and 13 weeks after adipose tissue transplantation. Results are shown as mean±SEM. There were no significant differences between groups at 6 (n=14-19 per group) or 13 weeks (n=7-9 per group). **E. Glucose tolerance.** Mice were fasted for 6 hours and injected intra-peritoneally with 2 g glucose/kg body weight. Glucose curves at each timepoint are shown in **Supplementary Figure 1**. Results are expressed as incremental areas under the curve (iAUC) between 0 and 120 min, and are shown as mean±SEM for each group. Differences between groups were assessed by one-way ANOVA. *$P<0.05$ vs. sham, † $P<0.01$ and ‡

P<0.05 vs. vis→vis. At 3, 6, 10 and 14 weeks after transplant, n=6-8, n=14-19, n=7-9 and n=7-9 mice for each group were studied, respectively.

Figure 2. Tissue-specific effects of adipose tissue transplantation. A. Changes in grafted fat mass after intra-abdominal transplantation. Results are shown as mean±SEM. Baseline results are taken from all 20 subQ→vis and 27 vis→vis mice. Numbers of mice are as follows: at 3 weeks, 6 subQ→vis and 8 vis→vis; at 6 weeks, 7 subQ→vis and 10 vis→vis; at 17 weeks, 7 subQ→vis and 9 vis→vis mice. **B. Changes in adipocyte size in grafted adipose tissue at 3, 6 and 17 weeks after transplantation.** The distribution of adipocyte cross-sectional area is shown as box-and-whisker plots (minimum to maximum, with the median and interquartile range shown). Differences between subQ and vis grafts were determined by Mann-Whitney test. **** P<0.0001 vs subQ→vis grafts. **C, E, G. Representative sections of subQ→vis adipose tissue grafts at 3, 6 and 17 weeks after transplantation, respectively.** Scale bar is 100μm. **D, F, H. Representative sections of vis→vis adipose tissue grafts at 3, 6 and 17 weeks after transplantation, respectively.** Scale bar is 100μm. **I. Leptin and PPAR-γ content in grafted fat.** Abbreviations: Ing, intact inguinal fat; Epi, intact epididymal fat; SubQ, subQ→vis graft; Vis, Vis→vis graft. **J. Plasma leptin concentrations at 3, 6, and 17 weeks after transplant.** Plasma leptin concentrations increased with time ($F_{2,56}$=24.82, P<0.0001, two-way ANOVA) but did not differ according to group ($F_{2,56}$=1.820, P=0.17). **K. Plasma adiponectin concentrations at 3, 6, and 17 weeks after transplant.** Plasma adiponectin concentrations tended to increase with time ($F_{2,58}$=3.05, P=0.055, two-way ANOVA), but were not different between groups ($F_{2,58}$=0.47, P=0.63).

Figure 3. Radiolabelled glucose tolerance test in chow and HFD-fed sham, subQ→vis and vis→vis mice. A. Masses of endogenous and grafted AT depots at 13 weeks post-transplantation. Differences between groups of mice were assessed by one-way ANOVA, with Dunn's post-tests for post-hoc comparisons. ** P<0.01 and *** P<0.001 vs. sham. **B. Plasma glucose concentrations during the radiolabelled GTT.** Plasma glucose concentrations are shown as mean±SEM. **C. Area under the plasma glucose curve.** Plasma glucose concentrations from 0 to 120 min were used to calculate the incremental area under the curve (iAUC) for each mouse. Results are shown as mean±SEM. * P<0.05 vs. sham; † P<0.05 vs. vis→vis. **D. Fasting plasma insulin concentrations prior to the GTT.** Results are shown as mean±SEM; * P<0.05 vs. sham. **E. Suppression of plasma free fatty acid concentrations.** Results are shown as mean±SEM. The difference between groups was not statistically significant by two-way ANOVA (effect of time: $F_{(1,34)}$=10.68, P=0.0025; effect of type of transplant: $F_{(3,34)}$ =1.12, P=0.35). **F. Radiolabelled glucose uptake in skeletal muscle and AT depots.** Results are shown as mean±SEM. * P<0.05, ** P<0.01, *** P<0.001 and **** P<0.0001 vs. sham.

Figure 4. Gene expression analysis of grafted subcutaneous AT reveals an induction of skeletal muscle-specific genes in both subQ→vis grafts and the endogenous inguinal depot of subQ→vis mice. A. Endogenous and transplanted AT depots selected for gene expression analysis. Gene expression was compared in five separate depots from three different experimental groups of mice: mice receiving an intra-abdominal graft of inguinal subcutaneous AT (subQ→vis), sham-operated mice (sham), and mice receiving a graft of inguinal subcutaneous AT in the dorsal subcutaneous space (subQ→subQ) (19). In subQ→vis mice, gene expression was measured in the grafted AT and two endogenous

depots (epididymal and inguinal). These depots were compared to endogenous inguinal subcutaneous AT from sham mice, and the grafted inguinal subcutaneous AT from subQ→subQ mice. **B. Skeletal muscle-specific genes, including several targets of MEF2A were selectively induced in both subQ→vis grafts and the endogenous inguinal subcutaneous AT of subQ→vis mice.** Genes displaying a >5-fold increase in expression (relative to grafted subQ→subQ AT) are listed, from highest to lowest. Genes that were selectively increased in both subQ→vis grafts and the endogenous inguinal subcutaneous AT of subQ→vis mice are highlighted in green. Predicted targets of MEF2A are indicated with an asterisk. **C. Expression of MEF2 subtypes in transplanted and intact fat pads.** MEF2D and MEF2D were selectively increased in expression in the endogeous inguinal depot of subQ→vis mice ($q<0.005$ vs. either subQ→vis EPI or sham ING). **D. Adipocyte cross-sectional area in the endogenous inguinal depot of sham, subQ→vis and vis→vis mice.** Results are shown as mean±SEM, n=7-9 per group.

Figure 5. SubQ→vis transplantation protects mice against HFD-induced hepatic TG accumulation. A. Hepatic TG content. TG content was determined in ~40 mg samples of liver using a colorimetric assay and Precimat glycerol standards (Roche Diagnostics, Mannheim, Germany). † $P<0.05$ vs. vis→vis mice. **B and C. Hepatic SREBP1 protein expression.** Livers from vis→vis mice displayed a tendency towards greater expression of SREBP1 relative to sham and subQ→vis mice ($P=0.12$). **D. Nominally-significant differences in gene expression, normalised to expression in livers from sham mice.** *$P<0.05$ vis→vis vs. subQ→vis and † $P<0.05$ vs. sham. **E. Immunoblot for proteins encoded by differentially-expressed genes.** Western blots for hepatic STAT3, SOCS3, LPL, ADIPOR2 and 14-3-3 (loading control).

Figure 6. Plasma cytokine concentrations at 4 and 10 weeks post-transplantation. Cytokines were measured using Bio-Plex Pro Mouse Cytokine Assay. Differences between groups were assessed by two-way repeated measures ANOVA. Those cytokines displaying significant differences between groups at either 4 or 10 weeks post-transplantation are shown. The remainder are shown in **Supplementary Table 5.** **P*<0.05 vs. sham; † *P*<0.05 vs. vis→vis.

Figure 7. Relationships between plasma cytokine concentrations, glucose tolerance and insulinaemia in chow and HFD-fed sham, subQ→vis, and vis→vis mice. A. Correlations between individual cytokines at 10 weeks post-transplantation and either incremental area under the curve during a glucose tolerance test (iAUC GTT) or fasting insulinaemia at 13 weeks. Correlations were performed in 40 mice (10 chow, 12 HFD sham, 8 subQ→vis and 10 vis→vis) using either Pearson correlation (for normally-distributed variables) or Spearman rank correlation (for variables not normally distributed). **B. Correlation between plasma TNF-α concentrations at 10 weeks post-transplant and iAUC GTT at 13 weeks.** Symbols are defined in the legend. **C. Correlation between plasma IL-17 concentrations at 10 weeks post-transplant and iAUC GTT at 13 weeks.**

REFERENCES:

1. **Vague J** 1956 The degree of masculine differentiation of obesities: a factor determining predisposition to diabetes, atherosclerosis, gout, and uric calculous disease. Am J Clin Nutr 4:20-34
2. **Kissebah AH, Krakower GR** 1994 Regional adiposity and morbidity. Physiol Rev 74:761-811
3. **Carr DB, Utzschneider KM, Hull RL, Kodama K, Retzlaff BM, Brunzell JD, Shofer JB, Fish BE, Knopp RH, Kahn SE** 2004 Intra-abdominal fat is a major determinant of the National Cholesterol Education Program Adult Treatment Panel III criteria for the metabolic syndrome. Diabetes 53:2087-2094
4. **Bjorntorp P** 1990 "Portal" adipose tissue as a generator of risk factors for cardiovascular disease and diabetes. Arteriosclerosis 10:493-496
5. **Nielsen S, Guo Z, Johnson CM, Hensrud DD, Jensen MD** 2004 Splanchnic lipolysis in human obesity. J Clin Invest 113:1582-1588
6. **Hocking S, Samocha-Bonet D, Milner KL, Greenfield JR, Chisholm DJ** 2013 Adiposity and insulin resistance in humans: the role of the different tissue and cellular lipid depots. Endocr Rev 34:463-500
7. **Perrini S, Laviola L, Cignarelli A, Melchiorre M, De Stefano F, Caccioppoli C, Natalicchio A, Orlando MR, Garruti G, De Fazio M, Catalano G, Memeo V, Giorgino R, Giorgino F** 2008 Fat depot-related differences in gene expression, adiponectin secretion, and insulin action and signalling in human adipocytes differentiated in vitro from precursor stromal cells. Diabetologia 51:155-164
8. **Manolopoulos KN, Karpe F, Frayn KN** 2010 Gluteofemoral body fat as a determinant of metabolic health. Int J Obes (Lond) 34:949-959
9. **Frayn KN** 2002 Adipose tissue as a buffer for daily lipid flux. Diabetologia 45:1201-1210
10. **Goodpaster BH, Kelley DE, Wing RR, Meier A, Thaete FL** 1999 Effects of weight loss on regional fat distribution and insulin sensitivity in obesity. Diabetes 48:839-847
11. **Pinnick KE, Nicholson G, Manolopoulos KN, McQuaid SE, Valet P, Frayn KN, Denton N, Min JL, Zondervan KT, Fleckner J, McCarthy MI, Holmes CC, Karpe F** 2014 Distinct Developmental Profile of Lower-Body Adipose Tissue Defines Resistance Against Obesity-Associated Metabolic Complications. Diabetes
12. **Xu H, Barnes GT, Yang Q, Tan G, Yang D, Chou CJ, Sole J, Nichols A, Ross JS, Tartaglia LA, Chen H** 2003 Chronic inflammation in fat plays a crucial role in the development of obesity-related insulin resistance. J Clin Invest 112:1821-1830
13. **Sun S, Ji Y, Kersten S, Qi L** 2012 Mechanisms of inflammatory responses in obese adipose tissue. Annu Rev Nutr 32:261-286
14. **Weisberg SP, McCann D, Desai M, Rosenbaum M, Leibel RL, Ferrante AW, Jr.** 2003 Obesity is associated with macrophage accumulation in adipose tissue. J Clin Invest 112:1796-1808
15. **Lumeng CN, Bodzin JL, Saltiel AR** 2007 Obesity induces a phenotypic switch in adipose tissue macrophage polarization. J Clin Invest 117:175-184
16. **Osborn O, Olefsky JM** 2012 The cellular and signaling networks linking the immune system and metabolism in disease. Nat Med 18:363-374
17. **Fabbrini E, Cella M, McCartney SA, Fuchs A, Abumrad NA, Pietka TA, Chen Z, Finck BN, Han DH, Magkos F, Conte C, Bradley D, Fraterrigo G, Eagon JC, Patterson BW, Colonna M, Klein S** 2013 Association between specific adipose tissue CD4+ T-cell populations and insulin resistance in obese individuals. Gastroenterology 145:366-374 e361-363

18. **Goldfine AB, Fonseca V, Jablonski KA, Pyle L, Staten MA, Shoelson SE** 2010 The effects of salsalate on glycemic control in patients with type 2 diabetes: a randomized trial. Ann Intern Med 152:346-357
19. **Hocking SL, Chisholm DJ, James DE** 2008 Studies of regional adipose transplantation reveal a unique and beneficial interaction between subcutaneous adipose tissue and the intra-abdominal compartment. Diabetologia 51:900-902
20. **Konrad D, Rudich A, Schoenle EJ** 2007 Improved glucose tolerance in mice receiving intraperitoneal transplantation of normal fat tissue. Diabetologia 50:833-839
21. **Tran TT, Yamamoto Y, Gesta S, Kahn CR** 2008 Beneficial effects of subcutaneous fat transplantation on metabolism. Cell Metab 7:410-420
22. **Rytka JM, Wueest S, Schoenle EJ, Konrad D** 2011 The portal theory supported by venous drainage-selective fat transplantation. Diabetes 60:56-63
23. **Foster MT, Shi H, Softic S, Kohli R, Seeley RJ, Woods SC** 2011 Transplantation of non-visceral fat to the visceral cavity improves glucose tolerance in mice: investigation of hepatic lipids and insulin sensitivity. Diabetologia 54:2890-2899
24. **Ohman MK, Shen Y, Obimba CI, Wright AP, Warnock M, Lawrence DA, Eitzman DT** 2008 Visceral adipose tissue inflammation accelerates atherosclerosis in apolipoprotein E-deficient mice. Circulation 117:798-805
25. **Foster MT, Softic S, Caldwell J, Kohli R, de Kloet AD, Seeley RJ** 2013 Subcutaneous Adipose Tissue Transplantation in Diet-Induced Obese Mice Attenuates Metabolic Dysregulation While Removal Exacerbates It. Physiol Rep 1
26. **Gunawardana SC, Piston DW** 2012 Reversal of type 1 diabetes in mice by brown adipose tissue transplant. Diabetes 61:674-682
27. **Stanford KI, Middelbeek RJ, Townsend KL, An D, Nygaard EB, Hitchcox KM, Markan KR, Nakano K, Hirshman MF, Tseng YH, Goodyear LJ** 2013 Brown adipose tissue regulates glucose homeostasis and insulin sensitivity. J Clin Invest 123:215-223
28. **Hoehn KL, Turner N, Swarbrick MM, Wilks D, Preston E, Phua Y, Joshi H, Furler SM, Larance M, Hegarty BD, Leslie SJ, Pickford R, Hoy AJ, Kraegen EW, James DE, Cooney GJ** 2010 Acute or chronic upregulation of mitochondrial fatty acid oxidation has no net effect on whole-body energy expenditure or adiposity. Cell Metab 11:70-76
29. **Bruce KD, Sihota KK, Byrne CD, Cagampang FR** 2012 The housekeeping gene YWHAZ remains stable in a model of developmentally primed non-alcoholic fatty liver disease. Liver Int 32:1315-1321
30. **Cooney GJ, Lyons RJ, Crew AJ, Jensen TE, Molero JC, Mitchell CJ, Biden TJ, Ormandy CJ, James DE, Daly RJ** 2004 Improved glucose homeostasis and enhanced insulin signalling in Grb14-deficient mice. EMBO J 23:582-593
31. **Joe AW, Yi L, Even Y, Vogl AW, Rossi FM** 2009 Depot-specific differences in adipogenic progenitor abundance and proliferative response to high-fat diet. Stem Cells 27:2563-2570
32. **Munoz S, Franckhauser S, Elias I, Ferre T, Hidalgo A, Monteys AM, Molas M, Cerdan S, Pujol A, Ruberte J, Bosch F** 2010 Chronically increased glucose uptake by adipose tissue leads to lactate production and improved insulin sensitivity rather than obesity in the mouse. Diabetologia 53:2417-2430
33. **Lai CF, Ripperger J, Morella KK, Wang Y, Gearing DP, Horseman ND, Campos SP, Fey GH, Baumann H** 1995 STAT3 and STAT5B are targets of two different signal pathways activated by hematopoietin receptors and control transcription via separate cytokine response elements. J Biol Chem 270:23254-23257

34. **Sabio G, Das M, Mora A, Zhang Z, Jun JY, Ko HJ, Barrett T, Kim JK, Davis RJ** 2008 A stress signaling pathway in adipose tissue regulates hepatic insulin resistance. Science 322:1539-1543
35. **Winer S, Paltser G, Chan Y, Tsui H, Engleman E, Winer D, Dosch HM** 2009 Obesity predisposes to Th17 bias. Eur J Immunol 39:2629-2635
36. **Patsouris D, Li PP, Thapar D, Chapman J, Olefsky JM, Neels JG** 2008 Ablation of CD11c-positive cells normalizes insulin sensitivity in obese insulin resistant animals. Cell Metab 8:301-309
37. **Jiao P, Chen Q, Shah S, Du J, Tao B, Tzameli I, Yan W, Xu H** 2009 Obesity-related upregulation of monocyte chemotactic factors in adipocytes: involvement of nuclear factor-kappaB and c-Jun NH2-terminal kinase pathways. Diabetes 58:104-115
38. **Yepuru M, Eswaraka J, Kearbey JD, Barrett CM, Raghow S, Veverka KA, Miller DD, Dalton JT, Narayanan R** 2010 Estrogen receptor-{beta}-selective ligands alleviate high-fat diet- and ovariectomy-induced obesity in mice. J Biol Chem 285:31292-31303
39. **Sell H, Habich C, Eckel J** 2012 Adaptive immunity in obesity and insulin resistance. Nat Rev Endocrinol 8:709-716
40. **Nishimura S, Manabe I, Nagasaki M, Eto K, Yamashita H, Ohsugi M, Otsu M, Hara K, Ueki K, Sugiura S, Yoshimura K, Kadowaki T, Nagai R** 2009 CD8+ effector T cells contribute to macrophage recruitment and adipose tissue inflammation in obesity. Nat Med 15:914-920
41. **Kintscher U, Hartge M, Hess K, Foryst-Ludwig A, Clemenz M, Wabitsch M, Fischer-Posovszky P, Barth TF, Dragun D, Skurk T, Hauner H, Bluher M, Unger T, Wolf AM, Knippschild U, Hombach V, Marx N** 2008 T-lymphocyte infiltration in visceral adipose tissue: a primary event in adipose tissue inflammation and the development of obesity-mediated insulin resistance. Arterioscler Thromb Vasc Biol 28:1304-1310
42. **Nov O, Shapiro H, Ovadia H, Tarnovscki T, Dvir I, Shemesh E, Kovsan J, Shelef I, Carmi Y, Voronov E, Apte RN, Lewis E, Haim Y, Konrad D, Bashan N, Rudich A** 2013 Interleukin-1beta regulates fat-liver crosstalk in obesity by auto-paracrine modulation of adipose tissue inflammation and expandability. PLoS One 8:e53626
43. **Zuniga LA, Shen WJ, Joyce-Shaikh B, Pyatnova EA, Richards AG, Thom C, Andrade SM, Cua DJ, Kraemer FB, Butcher EC** 2010 IL-17 regulates adipogenesis, glucose homeostasis, and obesity. J Immunol 185:6947-6959
44. **Harley IT, Stankiewicz TE, Giles DA, Softic S, Flick LM, Cappelletti M, Sheridan R, Xanthakos SA, Steinbrecher KA, Sartor RB, Kohli R, Karp CL, Divanovic S** 2014 IL-17 signaling accelerates the progression of nonalcoholic fatty liver disease in mice. Hepatology 59:1830-1839
45. **Jagannathan-Bogdan M, McDonnell ME, Shin H, Rehman Q, Hasturk H, Apovian CM, Nikolajczyk BS** 2011 Elevated proinflammatory cytokine production by a skewed T cell compartment requires monocytes and promotes inflammation in type 2 diabetes. J Immunol 186:1162-1172
46. **Goossens GH, Blaak EE, Theunissen R, Duijvestijn AM, Clement K, Tervaert JW, Thewissen MM** 2012 Expression of NLRP3 inflammasome and T cell population markers in adipose tissue are associated with insulin resistance and impaired glucose metabolism in humans. Mol Immunol 50:142-149
47. **Ognjanovic S, Jacobs DR, Steinberger J, Moran A, Sinaiko AR** 2013 Relation of chemokines to BMI and insulin resistance at ages 18-21. Int J Obes (Lond) 37:420-423

48. **Caspar-Bauguil S, Cousin B, Galinier A, Segafredo C, Nibbelink M, Andre M, Casteilla L, Penicaud L** 2005 Adipose tissues as an ancestral immune organ: site-specific change in obesity. FEBS Lett 579:3487-3492
49. **Paz-Filho G, Mastronardi CA, Parker BJ, Khan A, Inserra A, Matthaei KI, Ehrhart-Bornstein M, Bornstein S, Wong ML, Licinio J** 2013 Molecular pathways involved in the improvement of non-alcoholic fatty liver disease. J Mol Endocrinol 51:167-179

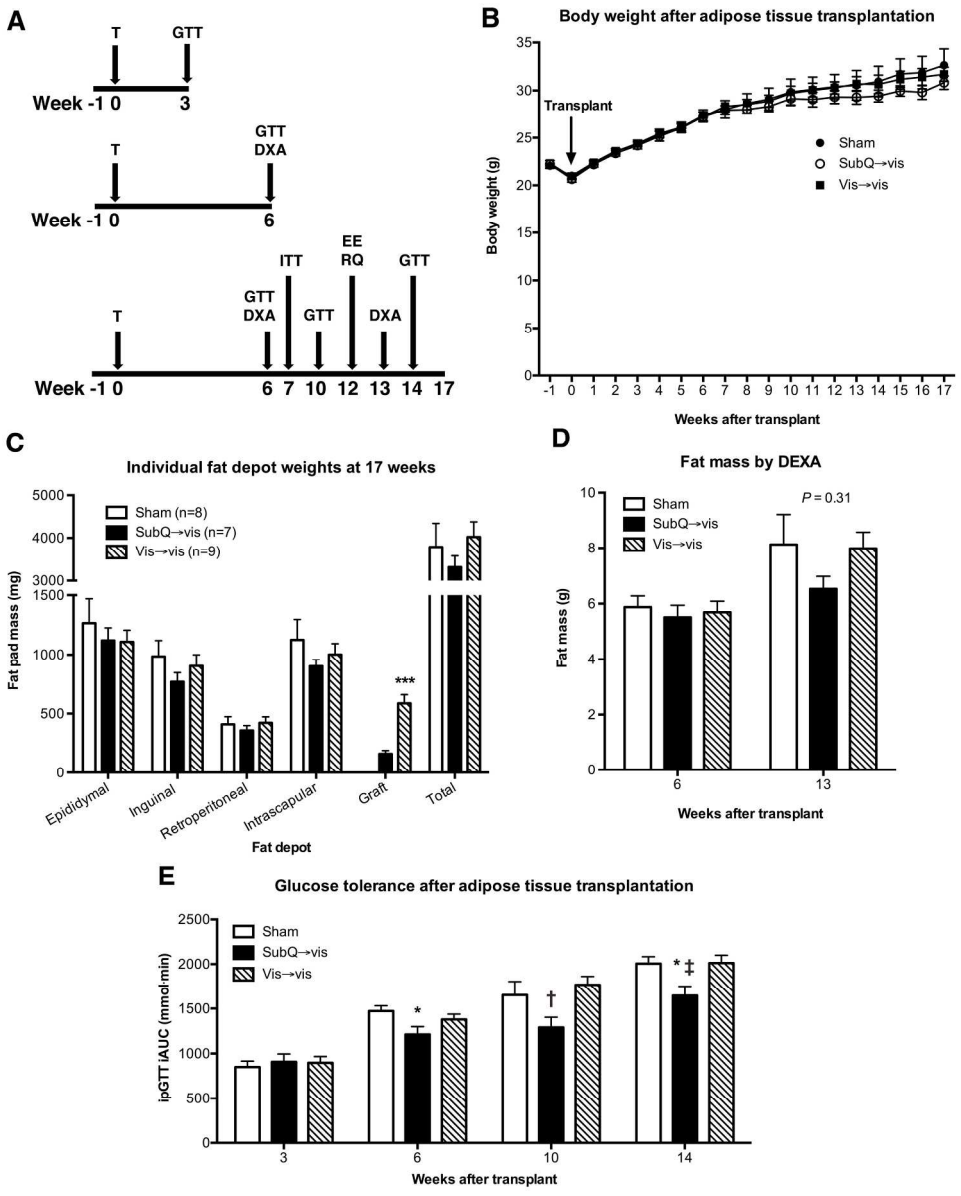

Figure 1. Whole-body effects of intra-abdominal adipose tissue transplantation.
219x268mm (300 x 300 DPI)

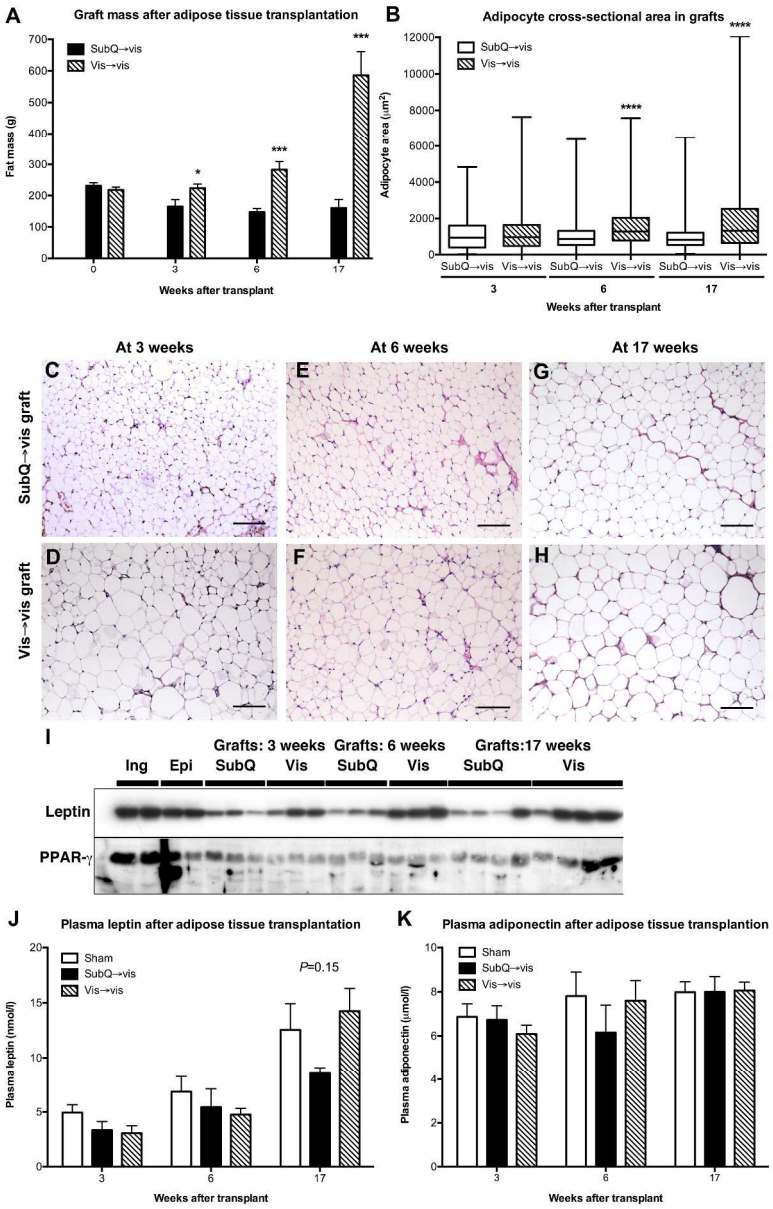

Figure 2. Tissue-specific effects of adipose tissue transplantation.
279x435mm (300 x 300 DPI)

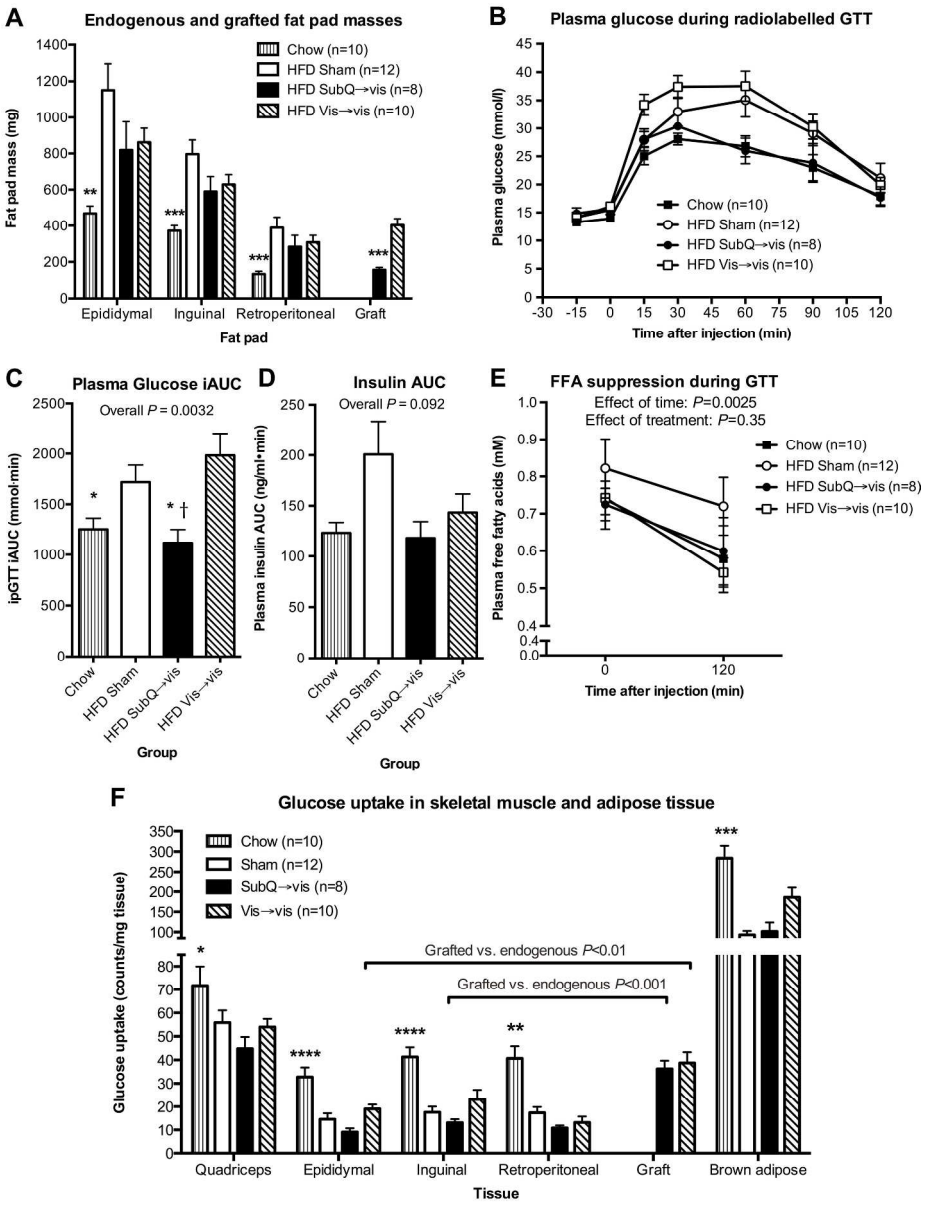

Figure 3. Radiolabelled glucose tolerance test in chow and HFD-fed sham, subQ→vis and vis→vis mice.
234x306mm (300 x 300 DPI)

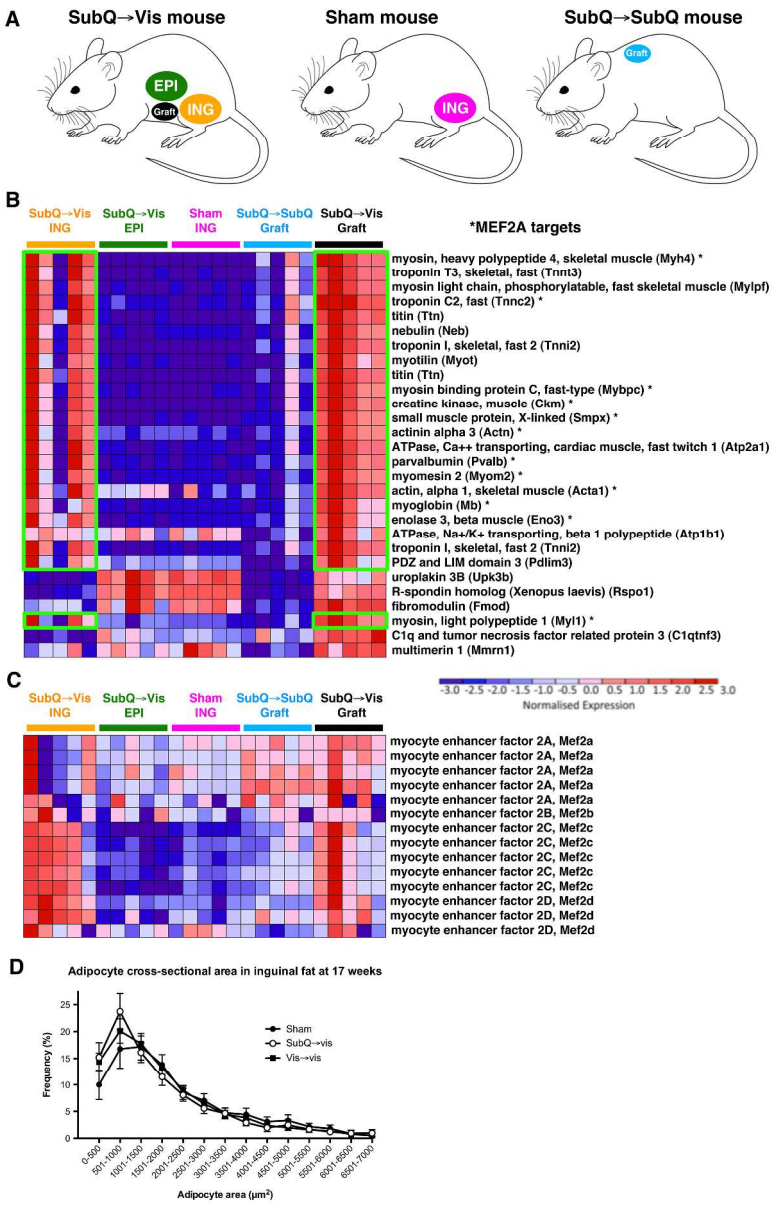

Figure 4. Gene expression analysis of grafted subcutaneous AT reveals an induction of skeletal muscle-specific genes in both subQ→vis grafts and the endogenous inguinal depot of subQ→vis mice.
279x435mm (300 x 300 DPI)

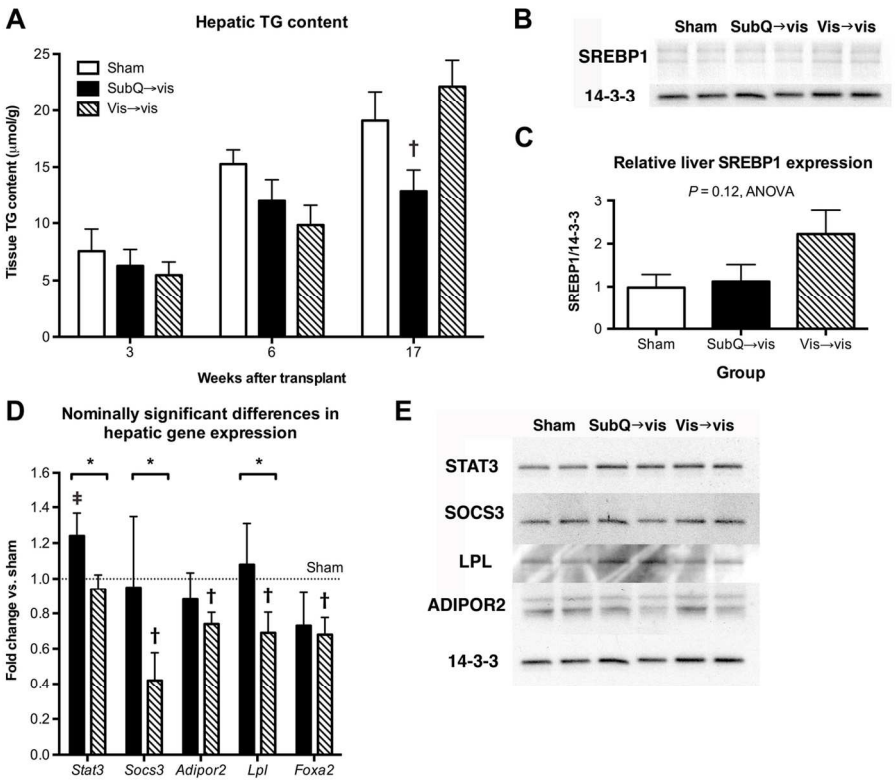

Figure 5. SubQ→vis transplantation protects mice against HFD-induced hepatic TG accumulation.
139x108mm (300 x 300 DPI)

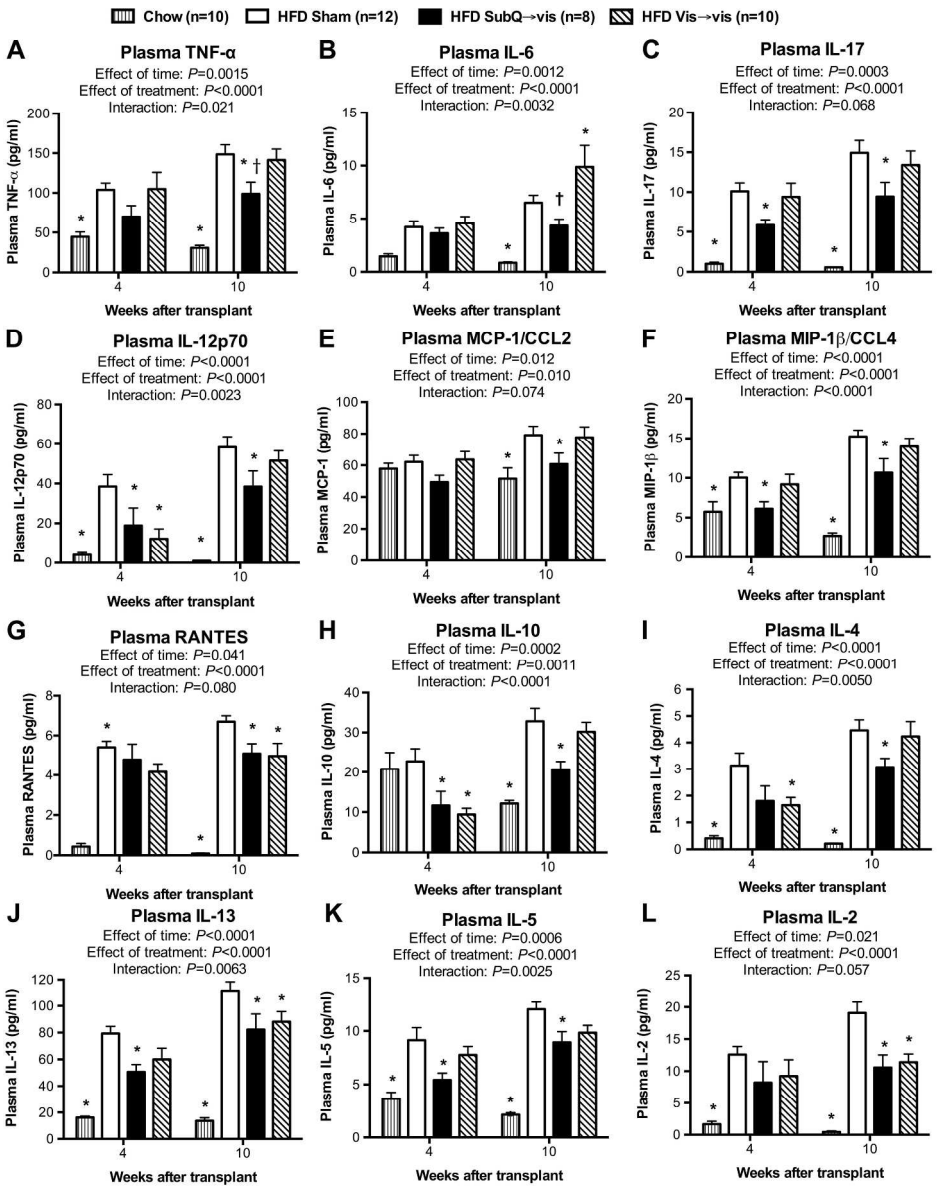

Figure 6. Plasma cytokine concentrations at 4 and 10 weeks post-transplantation.
229x293mm (300 x 300 DPI)

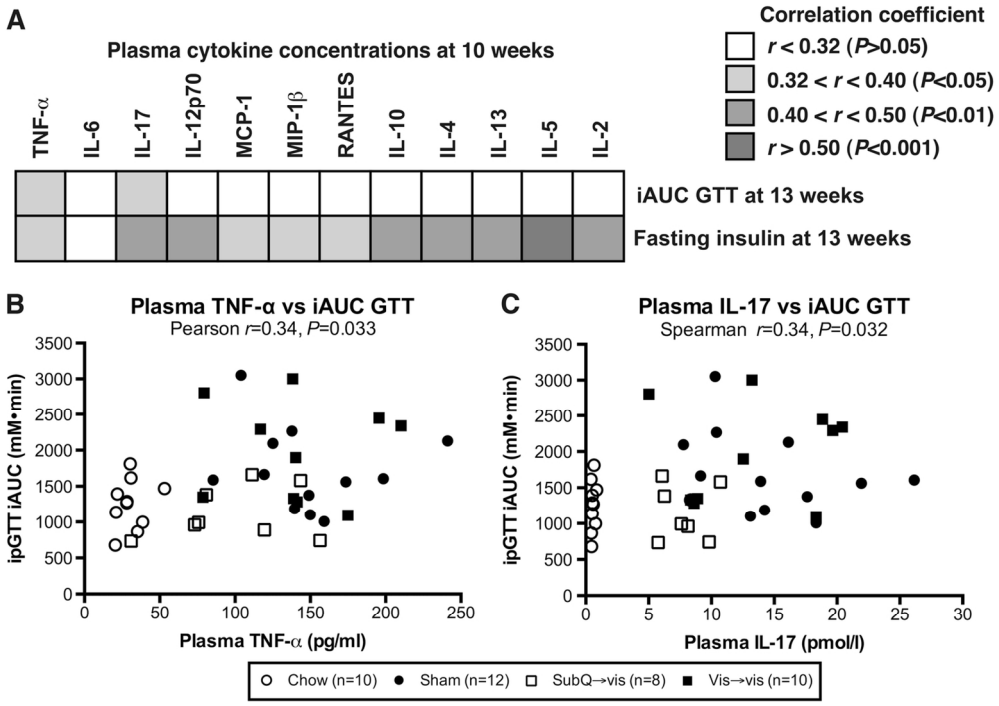

Figure 7. Relationships between plasma cytokine concentrations, glucose tolerance and insulinaemia in chow and HFD-fed sham, subQ→vis, and vis→vis mice.
128x91mm (300 x 300 DPI)

Supplementary Information for Hocking SL *et al.* "Subcutaneous fat transplantation alleviates diet-induced glucose intolerance and inflammation in mice"

Supplementary Methods:

Energy expenditure and body composition: Respirometry was determined as described in (1). Body composition was assessed by dual-energy x-ray absorptiometry (Lunar PIXImus, GE Medical Systems, New York, NY, U.S.A.) under isoflurane (2-2.5%) anaesthesia. Analysis was constrained to the body and limbs.

Tissues for immunoblotting: Tissues were homogenized in RIPA buffer **(**65 mM Tris·HCl, 150 mM NaCl, 5 mM EDTA, 1% NP-40, 0.5% Na deoxycholate, 0.1% SDS, and 10% glycerol, pH 7.4) containing 1 μg/ml aprotinin, 1 μg/ml leupeptin, 10 mM NaF, 1 mM Na_3VO_4, and 1 mM PMSF and incubated at 4°C for 2 h with agitation.

Intraperitonal insulin tolerance tests: Mice were fasted for four hours and basal blood glucose samples were obtained. This was followed by an intraperitoneal injection of 0.75 U/kg human insulin (Actrapid, Novo Nordisk, Baulkham Hills, Australia). Blood samples were taken from the tail vein at 0, 15, 30, 45, 60 and 90 min afterwards, and blood glucose was measured as above.

Indirect calorimetry and food intake: At 12 weeks after transplant, mice were housed individually in metabolic cages for 48 hours (Oxymax, Columbus Instruments, Columbus, OH, USA). Differences in energy expenditure between groups were assessed using a General Linear Model (SPSS software, IBM, St. Leonards, NSW,

Australia), with fat mass and fat-free mass entered as covariates (2). Food intake was measured by weighing food at the beginning and end of the 48-hour monitoring period.

Measurement of plasma cytokine concentrations: Cytokines measured included IL-1α, IL-1β, IL-2, IL-3, IL-4, IL-5, IL-6, IL-9, IL-10, IL-12(p40), IL-12(p70), IL-13, IL-17A, eotaxin, G-CSF, GM-CSF, IFN-γ, KC, MCP-1, MIP-1α, MIP-1β, RANTES and TNF-α.

Supplementary Figure 1. Blood glucose curves for intraperitoneal glucose tolerance tests performed at (A) 3, (B) 6, (C) 10 and (D) 14 weeks after transplantation. Mice were fasted for 6 hours and injected *i.p.* with 2 mg/kg of 50% glucose.

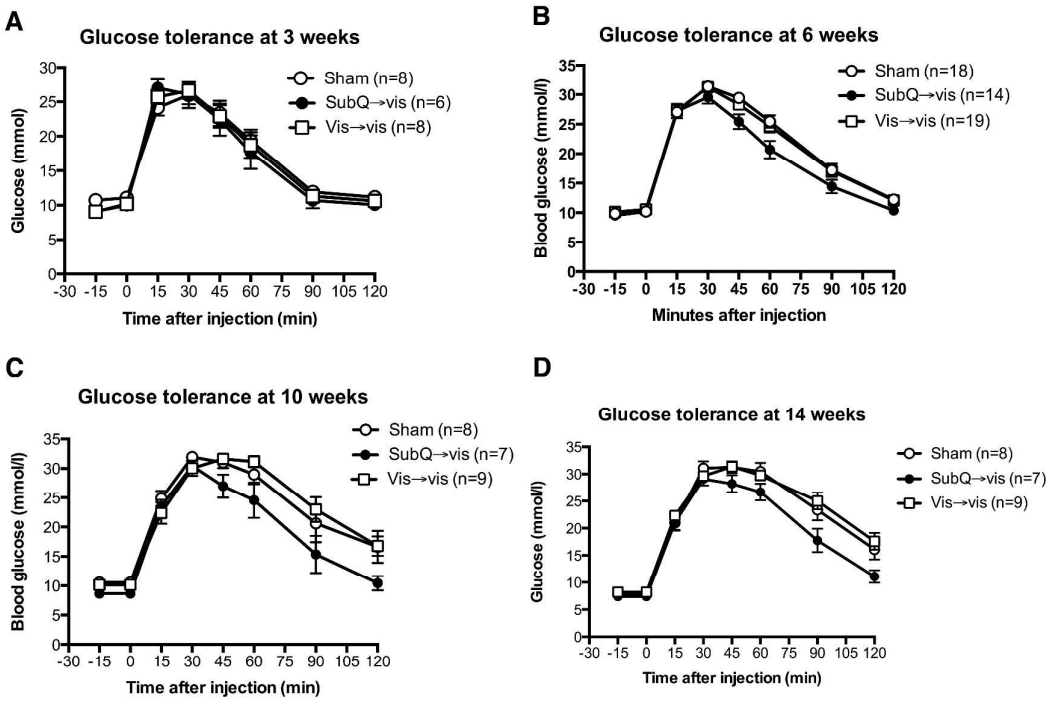

Supplementary Figure 2. Insulin tolerance test at 7 weeks after transplantation. Mice (n=7-9 for each group) were fasted for four hours. After measurement of basal blood glucose concentrations, mice were injected intraperitoneally with 0.75 U/kg human insulin. * $P<0.05$ and ** $P<0.01$, ANOVA.

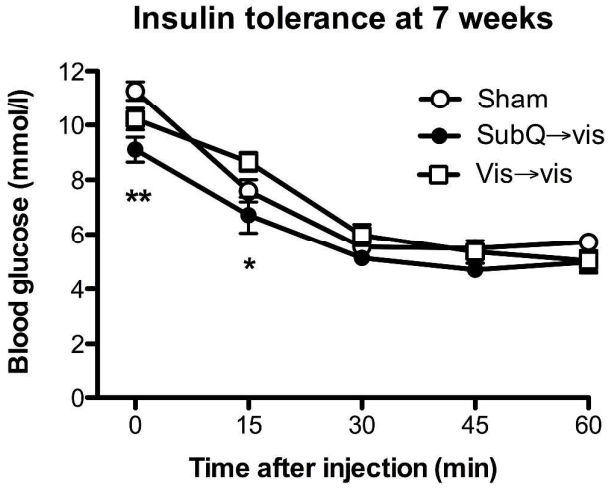

Supplementary Figure 3. Whole-body energy expenditure (heat) at 12 weeks after adipose tissue transplantation. Mice were acclimatised for 24 hours prior to measurements of energy expenditure and respiratory quotient using an Oxymax Instrument (Columbus Instruments). Results are shown as mean±SEM. When corrected for differences in body composition using ANCOVA (Supplementary Table 1 and reference (2)), there was no significant difference between groups (P<0.05).

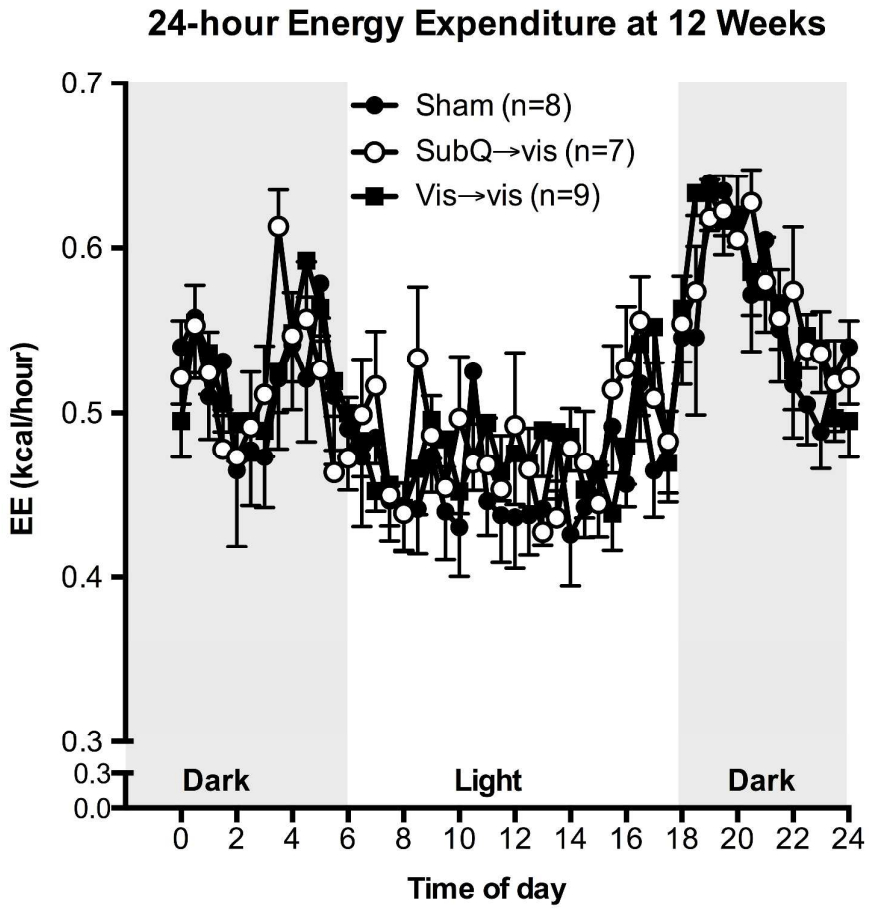

Supplementary Figure 4. Mean respiratory exchange ratio (RER) in light and dark phases at 12 weeks after adipose tissue transplantation. The differences between groups were not significant by two-way ANOVA (effect of phase: $F_{(1,21)}$=6.125, P=0.022; effect of type of transplant: $F_{(2,21)}$=0.54, P=0.59). The phase × interaction term was not significant ($F_{(2,21)}$=2.066, P=0.15).

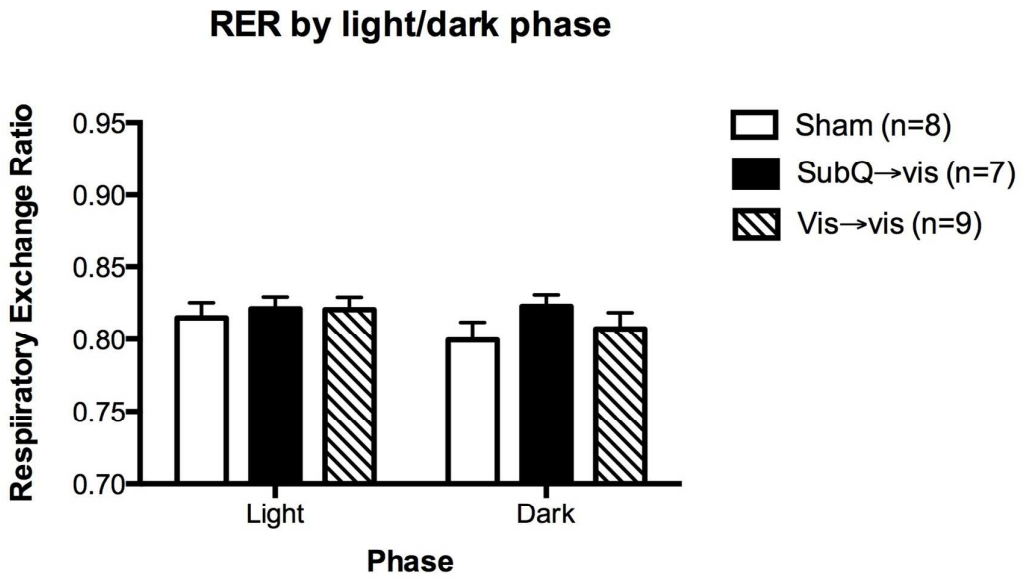

Supplementary Figure 5. Fed plasma lactate concentrations at 17 weeks post-transplantation. Results are shown as mean±SEM, n=7-9 per group. The difference between groups was not significant (overall *P*=0.24, ANOVA).

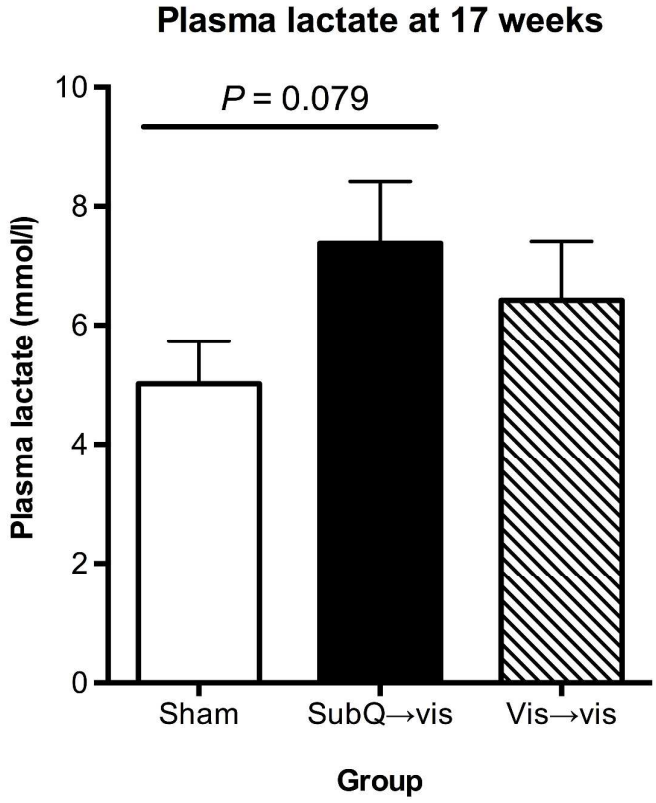

Supplementary Figure 6. Volcano plots (fold change vs. significance) for mRNA expression of 84 genes related to the pathogenesis of fatty liver and insulin resistance in sham, subQ→vis and vis→vis mice.

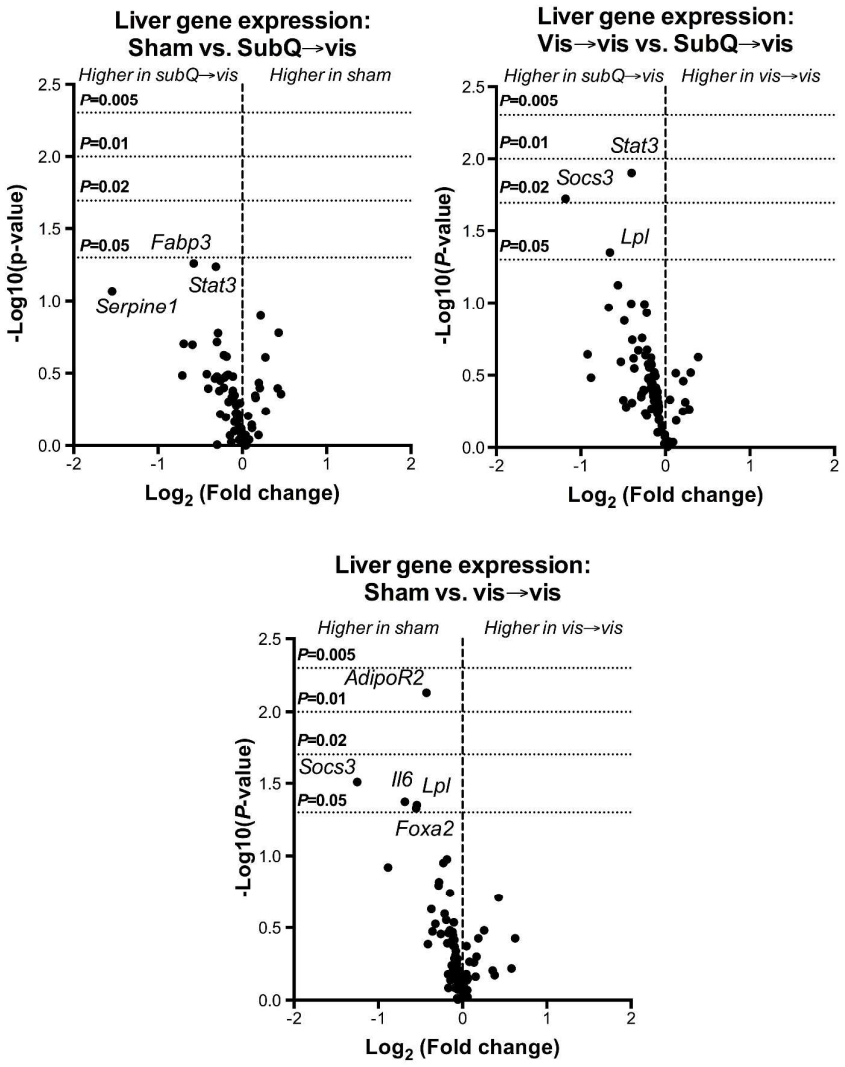

Supplementary Table 1. Energy expenditure and food intake measured at 12 weeks post-transplantation.

	Group			
	Sham (n=8)	*SubQ→vis* (n=7)	*Vis→vis* (n=9)	*P*
Energy expenditure (kcal/day)	12.1 ± 1.4	12.4 ± 0.6	12.4 ± 0.8	0.79
Body weight (g)	29.9 ± 1.3	29.0 ± 0.7	30.2 ± 0.7	0.68
Fat-free mass (g)	21.8 ± 0.4	21.9 ± 0.3	20.7 ± 0.4	0.043
Fat mass (g)	7.4 ± 1.2	5.8 ± 0.5	7.8 ± 0.7	0.30
Body fat (%)	24.4 ± 2.9	21.0 ± 1.6	27.0 ± 1.7	0.17
Food intake (kcal/day)	17.4 ± 1.3	19.3 ± 1.1	17.9 ± 1.3	0.57

Supplementary Table 2. List of 84 genes related to fatty liver examined by PCR array. Gene expression was measured using Mouse Fatty Liver RT^2 Profiler PCR Arrays (#330231 PAMM-157ZA, Qiagen, Doncaster, Victoria, Australia).

Unigene	GeneBank	Symbol	Description
Mm.277376	NM_013454	Abca1	ATP-binding cassette, sub-family A (ABC1), member 1
Mm.470747	NM_009593	Abcg1	ATP-binding cassette, sub-family G (WHITE), member 1
Mm.31374	NM_133360	Acaca	Acetyl-Coenzyme A carboxylase alpha
Mm.2445	NM_007381	Acadl	Acyl-Coenzyme A dehydrogenase, long-chain
Mm.282039	NM_134037	Acly	ATP citrate lyase
Mm.356689	NM_015729	Acox1	Acyl-Coenzyme A oxidase 1, palmitoyl
Mm.292056	NM_027976	Acsl5	Acyl-CoA synthetase long-chain family member 5
Mm.334199	NM_016870	Acsm3	Acyl-CoA synthetase medium-chain family member 3
Mm.259976	NM_028320	Adipor1	Adiponectin receptor 1
Mm.291826	NM_197985	Adipor2	Adiponectin receptor 2
Mm.6645	NM_009652	Akt1	Thymoma viral proto-oncogene 1
Mm.26743	NM_009692	Apoa1	Apolipoprotein A-I
Mm.221239	NM_009693	Apob	Apolipoprotein B
Mm.390161	NM_023114	Apoc3	Apolipoprotein C-III
Mm.305152	NM_009696	Apoe	Apolipoprotein E
Mm.12677	NM_020615	Atp5c1	ATP synthase, H+ transporting, mitochondrial F1 complex, gamma polypeptide 1
Mm.34405	NM_009810	Casp3	Caspase 3
Mm.406799	NM_007643	Cd36	CD36 antigen
Mm.439656	NM_009883	Cebpb	CCAAT/enhancer binding protein (C/EBP), beta
Mm.290251	NM_013493	Cnbp	Cellular nucleic acid binding protein
Mm.18522	NM_013495	Cpt1a	Carnitine palmitoyltransferase 1a, liver
Mm.307620	NM_009949	Cpt2	Carnitine palmitoyltransferase 2
Mm.21758	NM_021282	Cyp2e1	Cytochrome P450, family 2, subfamily e, polypeptide 1
Mm.57029	NM_007824	Cyp7a1	Cytochrome P450, family 7, subfamily a, polypeptide 1
Mm.491108	NM_026384	Dgat2	Diacylglycerol O-acyltransferase 2
Mm.22126	NM_017399	Fabp1	Fatty acid binding protein 1, liver
Mm.388886	NM_010174	Fabp3	Fatty acid binding protein 3, muscle and heart
Mm.741	NM_010634	Fabp5	Fatty acid binding protein 5, epidermal
Mm.1626	NM_007987	Fas	Fas (TNF receptor superfamily member 6)
Mm.236443	NM_007988	Fasn	Fatty acid synthase
Mm.938	NM_010446	Foxa2	Forkhead box A2
Mm.18064	NM_008061	G6pc	Glucose-6-phosphatase, catalytic
Mm.27210	NM_008062	G6pdx	Glucose-6-phosphate dehydrogenase X-linked
Mm.220358	NM_010292	Gck	Glucokinase
Mm.394930	NM_019827	Gsk3b	Glycogen synthase kinase 3 beta
Mm.246682	NM_008194	Gyk	Glycerol kinase
Mm.316652	NM_008255	Hmgcr	3-hydroxy-3-methylglutaryl-Coenzyme A reductase
Mm.202383	NM_008261	Hnf4a	Hepatic nuclear factor 4, alpha
Mm.240327	NM_008337	Ifng	Interferon gamma
Mm.268521	NM_010512	Igf1	Insulin-like growth factor 1
Mm.21300	NM_008341	Igfbp1	Insulin-like growth factor binding protein 1
Mm.874	NM_010548	Il10	Interleukin 10
Mm.222830	NM_008361	Il1b	Interleukin 1 beta

Mm.1019	NM_031168	Il6	Interleukin 6
Mm.268003	NM_010568	Insr	Insulin receptor
Mm.4952	NM_010570	Irs1	Insulin receptor substrate 1
Mm.3213	NM_010700	Ldlr	Low density lipoprotein receptor
Mm.259282	NM_010704	Lepr	Leptin receptor
Mm.1514	NM_008509	Lpl	Lipoprotein lipase
Mm.196581	NM_011949	Mapk1	Mitogen-activated protein kinase 1
Mm.21495	NM_016700	Mapk8	Mitogen-activated protein kinase 8
Mm.34213	NM_021455	Mlxipl	MLX interacting protein-like
Mm.21158	NM_020009	Mtor	Mechanistic target of rapamycin (serine/threonine kinase)
Mm.1103	NM_001033305	Ndufb6	NADH dehydrogenase (ubiquinone) 1 beta subcomplex, 6
Mm.256765	NM_008689	Nfkb1	Nuclear factor of kappa light polypeptide gene enhancer in B-cells 1, p105
Mm.968	NM_009473	Nr1h2	Nuclear receptor subfamily 1, group H, member 2
Mm.22690	NM_013839	Nr1h3	Nuclear receptor subfamily 1, group H, member 3
Mm.3095	NM_009108	Nr1h4	Nuclear receptor subfamily 1, group H, member 4
Mm.491140	NM_028994	Pck2	Phosphoenolpyruvate carboxykinase 2 (mitochondrial)
Mm.235547	NM_013743	Pdk4	Pyruvate dehydrogenase kinase, isoenzyme 4
Mm.260521	NM_008839	Pik3ca	Phosphatidylinositol 3-kinase, catalytic, alpha polypeptide
Mm.259333	NM_001024955	Pik3r1	Phosphatidylinositol 3-kinase, regulatory subunit, polypeptide 1 (p85 alpha)
Mm.383180	NM_013631	Pklr	Pyruvate kinase liver and red blood cell
Mm.28897	NM_026438	Ppa1	Pyrophosphatase (inorganic) 1
Mm.212789	NM_011144	Ppara	Peroxisome proliferator activated receptor alpha
Mm.328914	NM_011145	Ppard	Peroxisome proliferator activator receptor delta
Mm.3020	NM_011146	Pparg	Peroxisome proliferator activated receptor gamma
Mm.259072	NM_008904	Ppargc1a	Peroxisome proliferative activated receptor, gamma, coactivator 1 alpha
Mm.207004	NM_001013367	Prkaa1	Protein kinase, AMP-activated, alpha 1 catalytic subunit
Mm.277916	NM_011201	Ptpn1	Protein tyrosine phosphatase, non-receptor type 1
Mm.2605	NM_011255	Rbp4	Retinol binding protein 4, plasma
Mm.24624	NM_011305	Rxra	Retinoid X receptor alpha
Mm.267377	NM_009127	Scd1	Stearoyl-Coenzyme A desaturase 1
Mm.250422	NM_008871	Serpine1	Serine (or cysteine) peptidase inhibitor, clade E, member 1
Mm.10984	NM_009512	Slc27a5	Solute carrier family 27 (fatty acid transporter), member 5
Mm.21002	NM_011400	Slc2a1	Solute carrier family 2 (facilitated glucose transporter), member 1
Mm.18443	NM_031197	Slc2a2	Solute carrier family 2 (facilitated glucose transporter), member 2
Mm.10661	NM_009204	Slc2a4	Solute carrier family 2 (facilitated glucose transporter), member 4
Mm.3468	NM_007707	Socs3	Suppressor of cytokine signaling 3
Mm.278701	NM_011480	Srebf1	Sterol regulatory element binding transcription factor 1
Mm.38016	NM_033218	Srebf2	Sterol regulatory element binding factor 2
Mm.249934	NM_011486	Stat3	Signal transducer and activator of transcription 3
Mm.1293	NM_013693	Tnf	Tumor necrosis factor
Mm.469937	NM_013842	Xbp1	X-box binding protein 1
Mm.391967	NM_007393	Actb	Actin, beta
Mm.163	NM_009735	B2m	Beta-2 microglobulin
Mm.304088	NM_008084	Gapdh	Glyceraldehyde-3-phosphate dehydrogenase
Mm.3317	NM_010368	Gusb	Glucuronidase, beta
Mm.2180	NM_008302	Hsp90ab1	Heat shock protein 90 alpha (cytosolic), class B member 1

Supplementary Table 3. Non-significant changes in plasma cytokine concentrations at 4 and 10 weeks post-transplantation. Data are shown as mean±SEM. Differences between groups were assessed using two-way repeated measures ANOVA, and the two-tailed level of significance was $P<0.05$. This list contains cytokines that did not differ significantly between HFD-fed sham, subQ→vis and vis→vis mice. IFN-γ, MIP-1α and IL-9 were undetectable in the majority of samples. Abbreviations: ND, not detectable.

	4 weeks post-transplant				10 weeks post-transplant			
Plama Cytokine Concentration	Chow	HFD Sham	HFD SubQ→ vis	HFD Vis→vis	Chow	HFD Sham	HFD SubQ→ vis	HFD Vis→vis
N	10	12	8	9	10	12	8	9
IL-1α (pg/ml)	0.1±0.0	0.5±0.2	0.5±0.2	0.6±0.2	0.1±0.0	0.7±0.2	1.0±0.4	0.5±0.3
IL-1β (pg/ml)	74±14	86±10	71±15	94±12	36±16	109±10	84±9	94±9
IL-3 (pg/ml)	0.4±0.1	6.8±0.9	3.9±1.4	4.6±1.0	0.1±0.1	8.6±0.9	6.3±1.3	9.7±0.8
IL-12p40 (pg/ml)	24±5	80±7	68±7	89±9	15±2	84±9	73±6	88±10
Eotaxin	37±7	207±29	264±51	271±47	21±6	348±30	312±49	252±42
G-CSF	22±6	68±5	81±9	69±3	10±1	76±14	112±31	126±30
GM-CSF	ND	37±6	31±9	28±10	ND	71±8	56±8	76±9
KC	17±2	75±7	124±40	109±15	16±3	61±7	84±19	111±19

References:

1. **Hoehn KL, Turner N, Swarbrick MM, Wilks D, Preston E, Phua Y, Joshi H, Furler SM, Larance M, Hegarty BD, Leslie SJ, Pickford R, Hoy AJ, Kraegen EW, James DE, Cooney GJ** 2010 Acute or chronic upregulation of mitochondrial fatty acid oxidation has no net effect on whole-body energy expenditure or adiposity. Cell Metab 11:70-76
2. **Kaiyala KJ, Morton GJ, Leroux BG, Ogimoto K, Wisse B, Schwartz MW** 2010 Identification of body fat mass as a major determinant of metabolic rate in mice. Diabetes 59:1657-1666